



**Published in final edited form as:**

Fittolani, G., Seeberger, P. H., & Delbianco, M. (2020). Helical polysaccharides. *Peptide Science*, 112(1): e24124. doi:10.1002/pep2.24124.

## Helical polysaccharides

Giulio Fittolani, Peter H. Seeberger, Martina Delbianco



In analogy to polypeptides and polynucleotides, polysaccharides tend to form helical secondary structures, as well as higher hierarchical assemblies. Nevertheless, the conformation of polysaccharides in solution remains in most cases elusive due to their intrinsic complexity and lack of analytical techniques. In this review, we discuss the different helical shapes adopted by polysaccharides, with particular focus on how the helical character is exploited to form supramolecular assemblies, such as inclusion complexes with linear guest molecules and co-helices with polynucleotide strands. Several methodologies are used to tune the polysaccharides conformation, ranging from ion-mediated coil-helix transition to chemical synthesis of well-defined compounds with specific modifications. The latter provides ideal tailor-made probes for structural studies, with the aim to correlate their three-dimensional structure and the macroscopic properties. Applications of oligosaccharides with defined shapes in molecular recognition and catalysis are envisioned.

# Helical polysaccharides

Giulio Fittolani<sup>a</sup>, Peter H. Seeberger<sup>a,b</sup>, Martina Delbianco<sup>a\*</sup>

<sup>a</sup> Department of Biomolecular Systems, Max Planck Institute of Colloids and Interfaces, Am Mühlenberg 1, 14476 Potsdam, Germany

<sup>b</sup> Institute of Chemistry and Biochemistry, Freie Universität Berlin, Arnimallee 22, 14195 Berlin, Germany

\* Corresponding Author: [martina.delbianco@mpikg.mpg.de](mailto:martina.delbianco@mpikg.mpg.de)



## ABSTRACT

In analogy to polypeptides and polynucleotides, polysaccharides tend to form helical secondary structures, as well as higher hierarchical assemblies. Nevertheless, the conformation of polysaccharides in solution remains in most cases elusive due to their intrinsic complexity and lack of analytical techniques. In this review, we discuss the different helical shapes adopted by polysaccharides, with particular focus on how the helical character is exploited to form supramolecular assemblies, such as inclusion complexes with linear guest molecules and co-helices with polynucleotide strands. Several methodologies are used to tune the polysaccharides conformation, ranging from ion-mediated coil-helix transition to chemical synthesis of well-defined compounds with specific modifications. The latter provides ideal tailor-made probes for structural studies, with the aim to correlate their three-dimensional structure and the macroscopic properties. Applications of oligosaccharides with defined shapes in molecular recognition and catalysis are envisioned.

## KEYWORDS

Polysaccharides, Helix, Assemblies

## 1 INTRODUCTION

Polysaccharides are the most abundant biopolymers in nature, serving mainly as energy storage and structural materials. In addition, they are involved in several biological processes, such as cell recognition, differentiation, and adhesion.<sup>1</sup> Similarly to polypeptides and polynucleotides, polysaccharides adopt many regular conformations at the molecular level that strongly affect their properties and functions. Highly recurrent peptide secondary structures are  $\alpha$ -helices and  $\beta$ -sheets.<sup>2</sup> In analogy, helical and ribbon-like secondary structures with different degree of flexibility are widespread and have a great influence on the macroscopic properties of polysaccharides (Figure 1).<sup>3</sup> Nevertheless, the description of polysaccharides conformation and

folding dwarfs in comparison to polypeptides and often remains incomplete. Similarly, the principles governing their stability are not always well understood. The intrinsic complexity of polysaccharides posed a bottleneck, limiting the understanding of these biopolymers at the molecular level. Early work on polysaccharides produced a series of three-dimensional structures derived from X-ray diffraction of fibers. The conformation in solution, crucial to understand the biological functions of polysaccharides,<sup>4</sup> remained elusive due to lack of proper analytical techniques. The high structural diversity results from the different monosaccharide units (e.g. glucose, galactose, mannose) which can be substituted with multiple functional groups (e.g. acetyl, amine, sulfate). Such monosaccharides are linked with different connectivity (e.g. 1→3, 1→4, 1→6) through the glycosidic linkage, which can have different stereochemistry (i.e.  $\alpha$  or  $\beta$ ). The possibility to make branched structures increases the complexity of polysaccharides, when compared to linear polypeptides and polynucleotides (Figure 1). Moreover, the high flexibility, that makes polysaccharides very versatile macromolecules, hampered their study even further.

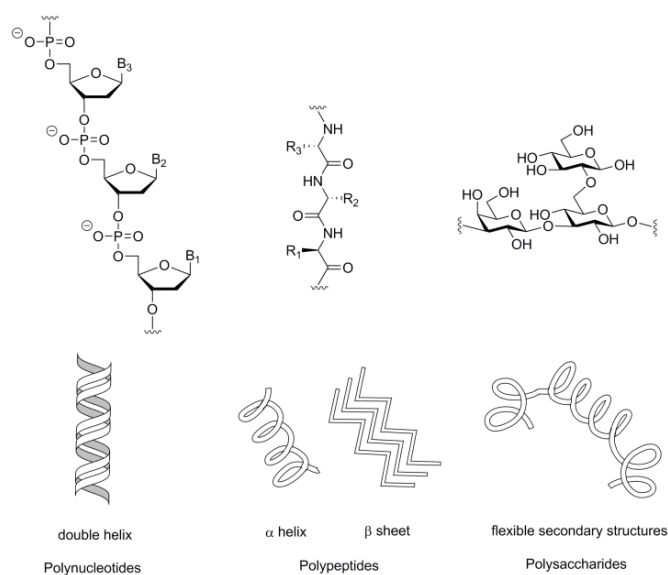


**Figure 1** Different classes of biopolymers based on different chemical linkages such as phosphodiester, amidic and glycosidic bond. A schematic representation of recurrent secondary structures for the different classes of biopolymers is shown.

Polysaccharide helices tend to interact with other materials in a highly recurrent manner, generating stable supramolecular assemblies. Furthermore, helical polysaccharides are particularly interesting for their strong tendency to form higher hierarchical structures, which often result in gel formation. Studying these structures can help to better understand polysaccharide properties, shedding light upon the forces that regulate polysaccharide interaction and aggregation. Herein, we review the different helical shapes adopted by polysaccharides in their native state, with special attention on the effect of the monosaccharide type and branching pattern on the conformation and macroscopic properties. We describe the most relevant methods used for structural elucidation, with particular emphasis on the most recent examples of solution phase studies. Several ways to influence helical stabilization are described, including co-assembly with other materials, ion-mediated coil-helix transition, as well

as chemical synthesis of tailor-made compounds with specific modification. Finally, the influence of the helical character over quaternary structure formation is described.

## 2 POLYSACCHARIDES THAT FORM HELICES

Helical conformations are common secondary structures for polypeptides, as well as for polysaccharides. Polypeptide helices are described with the standard  $X_n$  nomenclature in which  $X$  represents the number of residues per helical turn and  $n$  the number of atoms in the hydrogen-bonded loop. Differently, polysaccharide helical symmetry is commonly denoted using the  $U_v$  nomenclature with  $U$  representing the number of units in  $v$  helical turns.<sup>5</sup> From a biological standpoint, the helical arrangement is advantageous because it allows for efficient packing of molecules and thus high energy storage capabilities. A standard polypeptide  $\alpha$ -helix has 3.6 amino acids per turn, with a pitch of 5.4 Å. Polysaccharide helices are much more diverse, with a pitch range between 7 and 47 Å. Furthermore, the assembly of unimeric polysaccharide chains into higher hierarchical structures, such as tertiary and quaternary structures, is known, as described by multiple helical assemblies and gel networks of carrageenans, a class of sulfated polyelectrolyte polysaccharides.<sup>6</sup> The hollow helix is a highly recurrent local conformation of polysaccharides in which stabilization derives from non-covalent forces including hydrophobic interactions, hydrogen bonding, dipole, and ionic interactions.<sup>7</sup> A general feature of these helices is the hydrophobic character of the central cavity, generated by the axial C-H bonds of the sugar ring. On the contrary, the exterior is highly hydrophilic, due to the exposure of hydroxyl groups. The hydrophobic character of the internal void, together with interstrand hydrogen bonding, is crucial for the formation of higher hierarchical structures, such as helical inclusion complexes and double (or triple) helical assemblies. Many polysaccharides exist in a helical conformation only upon double or triple helix formation, switching to a random coil when the supramolecular assembly is disrupted (*i.e.* denaturation process). The external input, which can disrupt such structures, could be temperature or ionic strength. Furthermore, some polysaccharide helices showed a degree of flexibility adapting their size to the guest molecule (*i.e.* adapting the pitch ( $p$ ) and number of units per turn ( $n$ )).<sup>8</sup> Other commonly adopted secondary structures are extended ribbons, which are typically rigid and flat, with amphiphilic character.

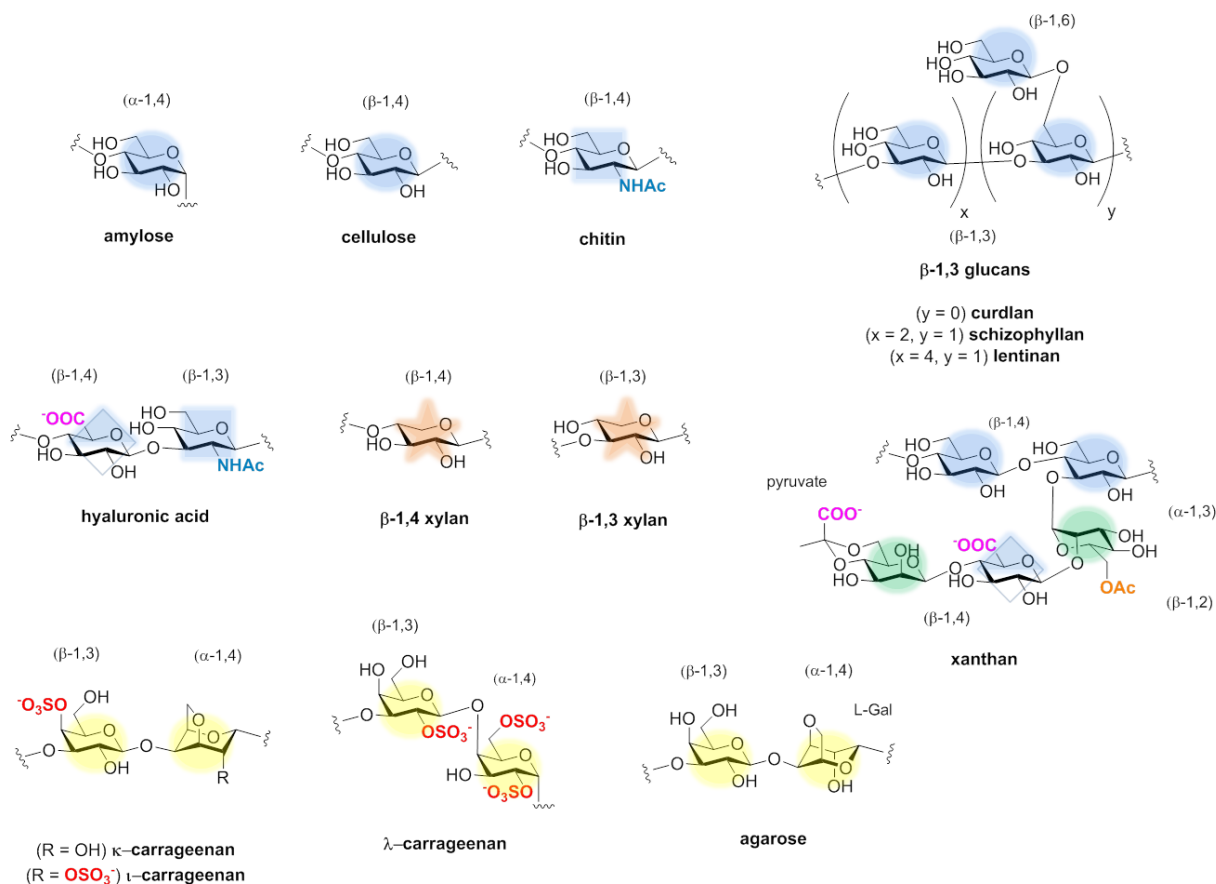


**Figure 2** Chemical structures of natural polysaccharides. The monosaccharides are represented following the Symbol Nomenclature for Glycans (SNFG).<sup>9</sup>

Amylose is the major representative of the polysaccharide hollow helix family (Figure 2) and adopts a double helical supramolecular structure with two left-handed  $6_1$  helices twisted around each other, in the crystalline form (Figure 3B). Two allomorphs (A and B) are reported for native amylose with similar chain conformation, but different crystalline packing of the double helices. The helical pitch of A and B amylose is respectively 21.4 and 20.8 Å. Even though no intramolecular hydrogen bonds are present, an extensive hydrogen bonding network exists between the two strands stabilizing the double helix. Additional stabilization results from van der Waals interactions. The interstrand association makes the central cavity too small to accommodate water molecules (inner diameter 3.5 Å, Figure 3B).<sup>10–12</sup> Beside these native allomorphs, a V-form, with a guest molecule in the central hydrophobic cavity (e.g. starch-iodine complex) exists. The V-form is a fairly flexible single  $6_1$  left-handed helix with the helical size that can adapt to the size of the guest molecule (Figure 3A); different inner diameters have been reported (4.5, 6.0 and up to 7–8 Å), while the pitch is approximately 8 Å. In contrast with the A and B forms, the V-form is stabilized by intramolecular hydrogen bonds.<sup>8,13–15</sup> The sugar rings are oriented in a parallel fashion with respect to the helix axis, thus creating a hydrophobic central void able to host molecules (Figure 3A).<sup>8,16</sup> A double helix with a central hydrophobic cavity was also observed for an amylose oligomer and polyiodide.<sup>13</sup> The conformation of amylose in solution is still under debate and a method to determine it unambiguously remains elusive.<sup>17</sup> An attempt to monitor the conformational changes in solution has been performed,

following the enzymatic synthesis of amylose with Small Angle X-ray Scattering (SAXS). Six-Fold double helices (21 Å pitch), as well as wormlike chains, were observed, depending on the length of amylose and on the synthetic conditions.<sup>18</sup>

$\beta$ -1,3 Glucans (Figure 2) are polysaccharides widespread in fungi, plants, bacteria, and yeast, serving structural function as components of the cell wall, as well as energy reserve function.<sup>19</sup> Most of them adopt hollow helical structures, usually arranging into triple helices. Curdlan, a linear  $\beta$ -1,3 polyglucoside (Figure 2), is the simplest polysaccharide of this family. The anhydrous form is partially crystalline, with a triple right handed helical structure made of three  $6_1$  strands, held together by hexagonal interstrand hydrogen bonding between hydroxyls in position 2 and hydrophobic interactions (pitch 18.78 Å, Figure 3C).<sup>20</sup> A double helical conformation appears as an intermediate during the curdlan denaturation process.<sup>21</sup> Schizophyllan (Figure 2) is based on the same linear backbone as curdlan having, in addition, a regular pattern of  $\beta$ -1,6 glucose branching every third residue. Similarly to curdlan, this polysaccharide shows a triple helical arrangement ( $6_1$  helices, pitch of 18 Å) stabilized by hydrogen bonds, while the glucose sidechains extend towards the outside.<sup>19,22</sup> Upon denaturation, a combination of hydrophobic interactions and H-bonds helps the reformation of the triple helices.<sup>23</sup> Lentinan, an analogue of schizophyllan with a regular pattern of  $\beta$ -1,6 glucose branching (Figure 2), also adopts a triple helical superstructure in its native form.<sup>20</sup> The presence of the sidechains in these  $\beta$ -1,3 glucans has a direct effect on macroscopic properties. Curdlan self-assembles to give water insoluble aggregates, while schizophyllan and lentinan are water soluble.<sup>24,25</sup>

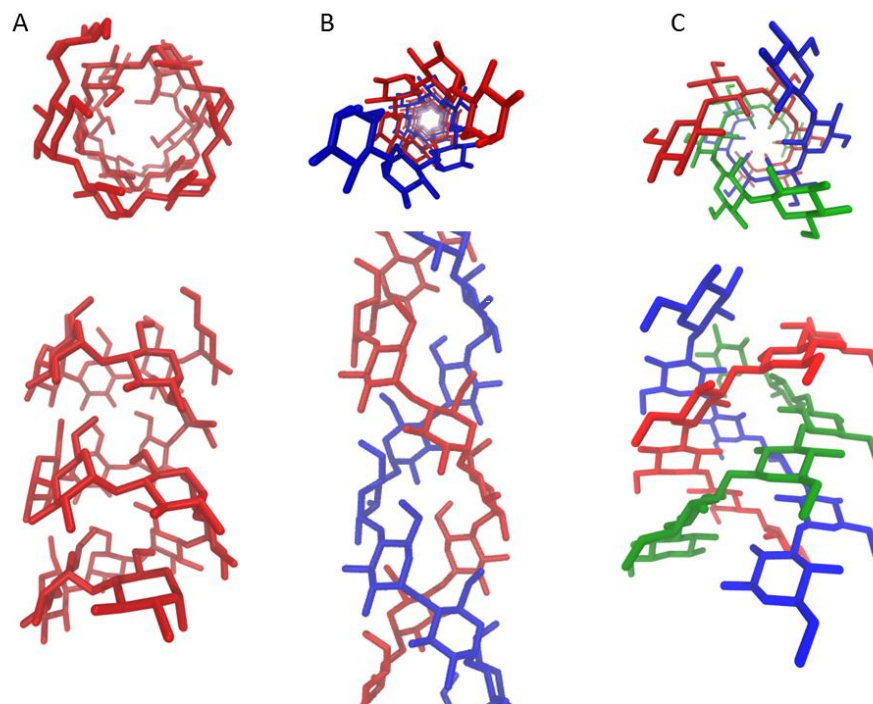


**Figure 3** Side and top view of single, double and triple helical polysaccharides. The helix symmetry is denoted by  $U_v$  which means that there are  $U$  repeat units in  $v$  turns of the helix. A) V-amylose left-handed  $6_1$  helix. B) A-amylose left-handed  $6_1$  double helix. C) Curdlan right-handed  $6_1$  triple helix.



Similar to  $\beta$ -glucans,  $\beta$ -1,3-xylans (Figure 2) adopt right-handed triple helical superstructures. Each helix has six xylopyranose units per turn with a 18.36 or 17.55 Å pitch, depending on the water content.<sup>26,27</sup> The recurrent feature of these  $\beta$ -1,3-glucans/xylans is the presence of a triad of hydrogen bonds between the hydroxyl groups in position 2 at the center of the triple helix. The orientation of the sugar rings is roughly perpendicular to the helical axis (characteristic of the screw helix) with the hydroxyl in position 6 pointing outwards (if present).

Most glycosaminoglycans (GAGs) have an alternating pattern of 1,3 and 1,4 glycosidic linkages. They exhibit a variety of single, left-handed helices with different degrees of extension, ranging from two to four folds. More complex arrangements, such as the  $8_5$  helices of chondroitin 6-sulfate and dermatan sulfate, were also detected.<sup>7</sup>

Hyaluronic acid (or hyaluronan) is a polyelectrolyte, bearing carboxylic acid moieties. Despite the simple disaccharide repetitive unit of hyaluronic acid (Figure 2) and the extensive use of this polysaccharides in the biomedical field, its solution conformation is still under debate.<sup>28</sup> In solid phase (*i.e.* fiber diffraction), hyaluronic acid shows high variety of allomorphs, adopting left-handed helical arrangements with 2, 3 and 4 repetitive units per turn (both single and double helical). The helical conformation in the solid state depends on many parameters, such as the counterion, pH, temperature and hydration. The ability to adopt a wide range of conformations makes hyaluronic acid a versatile biopolymer with several biological functions.<sup>28,29</sup> For instance, the presence of divalent cations (*i.e.*  $\text{Ca}^{2+}$ ) influences the structure, stabilizing a single threefold helical structure with a pitch of 28.4 Å and creating an ionic bridge between adjacent polyionic strands, whereas low pH favors a  $4_3$  double helical arrangement with 32.8 Å pitch.<sup>30,31</sup> It has been suggested that, in solution, this polysaccharide exists in a ordered conformation, in which each disaccharide repetitive unit is twisted by 180° with respect to the next unit. The twofold helix can be viewed as an extended ribbon stabilized by intrachain hydrogen bonds and able to form duplexes (*i.e.* interchain association), thanks to interactions between hydrophobic “patches”.<sup>28</sup>

Carrageenans (Figure 2) are a class of gel-forming, linear sulfated polysaccharides with a disaccharide galactan backbone, found in seaweed. Among them, iota and kappa-carrageenans adopt a random coil or right-handed single helical secondary structure depending on the ionic environment. X-ray fiber studies suggested a conformation based on a double helix with three disaccharide units per turn (threefold), with a pitch ranging from 26.0 to 24.6 Å. The stability of the double helix was thought to arise from interstrand hydrogen bonds buried in the helix interior, while the sulfate groups are pointing outwards.<sup>32</sup> Recently, AFM imaging proved their single stranded nature and their tendency to associate into supramolecular entities, responsible for gel network formation.<sup>6,33</sup>

Similar to carrageenans, agarose has a galactan backbone (Figure 2). The absence of sulfate groups and the L-anhydro galactose in the repetitive unit strongly affect the conformation. In contrast with carrageenans, agarose adopts a left handed double helical supramolecular arrangement, with three disaccharide units per turn and a shorter pitch (19.6 Å). The double helix has a small internal cavity 4.5 Å, with all the C-H bonds pointing towards the center. Its stability is not completely understood, since no hydrogen bonds are found to sustain the double helix.<sup>7,34</sup> As a result of unconventional fiber preparation, single helices of agarose have also been reported.<sup>35</sup>

Cellulose and chitin (Figure 2) adopt a rigid, flat, and extended ribbon secondary structure, stabilized by inter and intra strand hydrogen bonding, as well as by hydrophobic interaction. The aggregation of such polysaccharides leads to water insoluble materials.<sup>36</sup> The extended ribbon secondary structure can be viewed as a non-chiral  $2_1$  helix. Surprisingly  $\beta$ -1,4-xylans, which are very similar to cellulose in their primary structure but lack the typical O-3 O-5' intramolecular hydrogen bond of cellulose, exist as  $3_1$  left handed single helices with a pitch of 14.85 Å. The helical arrangement seems to be stabilized by interactions with water.<sup>37</sup>

Xanthan (Figure 2), a microbial polysaccharide, is based on a cellulose backbone with the addition of a charged trisaccharide side chain at every other glucose unit. Due to the presence of such branches, xanthan is water soluble and does not adopt the extended flat ribbon conformation typical of cellulose. Fiber X-ray diffraction studies suggested a  $5_1$  single helical structure, with a pitch of 47 Å (five cellobiose units per turn) and stabilization arising from packing of sidechains along the backbone. However, other studies suggested the formation of a double helical structure. The debate has been recently addressed with AFM imaging, revealing that xanthan follows a two-step organization process. A random coil conversion to single helix, followed by dimerization into an antiparallel  $5_1$  double helix, was observed in solution. Nevertheless, the experimental conditions (*i.e.* ionic strength or thermal treatment) can block the disorder-order transition at the single helical stage.<sup>38</sup>

### 3 METHODS TO STUDY POLYSACCHARIDE CONFORMATIONS AND FOLDING

The study of polysaccharide secondary structures, and higher hierarchical assemblies, has been hampered by the intrinsic complexity of polysaccharides. Even though several crystal structures were obtained with X-ray fiber diffraction, the geometry of many polysaccharides remains less well understood. In addition, the conformation that polysaccharides adopt in solution is often not known, since few techniques for solution studies are available. In many cases, the coexistence of ordered and disordered conformations limits the use of conventional techniques. The best results are generally obtained combining different techniques (*e.g.* NMR, Molecular Dynamics simulations, SAXS, and AFM). The complementary, rather than alternative methods used to study polysaccharide conformations and folding can be divided into three broad categories: i) diffraction techniques, ii) imaging techniques, and iii) spectroscopic techniques.

One of the most powerful diffraction techniques used to study polysaccharide crystal structures is fiber (or film) X-ray diffraction (XRD) analysis. Due to their nature, sufficiently large single crystals of polysaccharides are hard to obtain, whereas it is possible to prepare oriented fibers (*i.e.* all the helical axes are parallel to each other). The fiber diffraction pattern obtained, aided by modelling, can give information on the helix type (*i.e.* pitch and symmetry), on the possible formation of intertwining helices, as well as on the relative orientation (*i.e.* parallel/antiparallel).<sup>5,39</sup> A complementary technique is electron diffraction crystallography, which allows for the measurement of a diffraction pattern from small crystals, visible in TEM micrograph (Transmission Electron Microscopy).<sup>40</sup> To date, more than 150 polysaccharide structures have been solved with these techniques and the results are organized in a database (PolySac3DB).<sup>41</sup> Nevertheless, these methods have an intrinsic limitation, since they can only



reveal the conformation in solid phase. In addition, the sample preparation (fiber or film) greatly affects the helical arrangement.<sup>29</sup>

Small Angle X-ray Scattering (SAXS) has been widely used to extract low-resolution models of proteins.<sup>42</sup> This technique does not require a crystalline sample and can directly analyze the macromolecule in solution. Furthermore, SAXS can provide dynamic information on large conformational changes, occurring in solution. Radius of gyration ( $R_g$ ), mass, compactness, flexibility, and overall shape are important structural information accessible with SAXS. The comparison of the low-resolution SAXS model with high-resolution, atomically detailed models derived from other techniques (*i.e.* XRD, NMR, MD simulations) yields a clear image of the macromolecule in solution.<sup>42</sup> SAXS, in combination with MD simulations, has been recently applied to obtain information on a decasaccharide overall shape.<sup>43</sup> However, the need of collimated X-ray beams (*i.e.* synchrotron radiation) has limited the use of this technique.

Static Light Scattering (SLS) also provides information on the conformation in solution. As for SAXS, light scattering provides the radius of gyration and has been used to observe salt-induced “order-disorder” transition in polysaccharides.<sup>44</sup> Difficult sample preparation, due to the high aggregation tendency of polysaccharides, has limited the use of SLS. Moreover, this technique is only applicable to compounds longer than 10 nm and it cannot provide detailed information on secondary structure.

Among the imaging techniques, Atomic Force Microscopy (AFM) holds the most potential, due to its ability to directly visualize single polysaccharide molecules, with the significant advantage to operate in “near-native” conditions.<sup>45–48</sup> Statistical analysis of individual molecules allows for height, contour length, and persistence length ( $L_p$ ) measurements.<sup>49</sup> Moreover, AFM allows for polysaccharide flexibility determination. With this technique, it has been possible to follow secondary and tertiary structure formation of carrageenans, as a function of time or salt concentration.<sup>6,33,50,51</sup> Single Molecule Force Spectroscopy (SMFS) exploits the possibility to attach single molecules to the AFM tip, either by chemical conjugation or by non-specific interactions.<sup>52–55</sup> Once the molecule is coupled to the tip, mechanical manipulation is possible; the tip is moved away from the sample and a force-extension curve is derived (Figure 4A). Such curves provide information on mechanical properties of the single molecule and hence contain a fingerprint of the secondary structure of the polysaccharide (Figure 4B). Many polysaccharides single helices and supramolecular assemblies have been characterized using SMFS.<sup>21,52,53,56,57</sup>

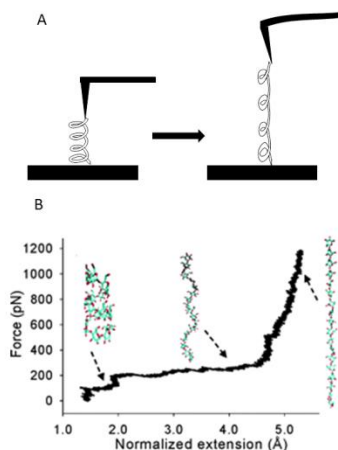


**Figure 4** A) Schematic representation of the SMFS used to study the force-induced unfolding of single polysaccharide helices. The tip is moved away from the sample and the single molecule is unfolded. B) A simulated force-extension curve for amylose in butanol. Reprinted with permission from<sup>56</sup>. Copyright 2006 American Chemical Society.

NMR techniques can be used to gain some information on the solution conformation. The Nuclear Overhauser Effect (NOE), which depends on the distance between two nuclei ( $\propto r^{-6}$ ), has been exploited to elucidate three-dimensional structures. However, the NOE short range (up to 4 Å) and large timescale (50 ms to 1 s) often produced uncertain results.<sup>58,59</sup> Other methods, such as measurement of Residual Dipolar Coupling (RDC), analyses of  $J$ -couplings across  $O$ -glycosidic linkages, and hydrogen bond studies are useful and more reliable tools.<sup>60–64</sup> In contrast to protein, the use of NMR suffers from the chemical shift degeneracy and intrinsic flexibility of polysaccharides. To overcome this issue, the introduction of isotopic labels<sup>60–62,65</sup> or paramagnetic lanthanide complexes<sup>66,67</sup> is sometimes exploited. However, generating a 3D structure solely from NMR data is rather difficult. The combination of NMR experiments with theoretical Molecular Dynamics (MD) simulations is often employed and provided important structural information.<sup>61,68–74</sup>

Most methods to study polysaccharide conformation are adapted from protein and peptide structural analysis. However, many polysaccharides have a high tendency to form gels and require unconventional means of analysis. Raman Optical Activity (ROA) allows for direct observation of highly hierarchical structures by monitoring the difference in Stokes scattering intensity of right and left circularly polarized light, thus introducing sensitivity for asymmetry and chirality. This technique has been used to determine the secondary structure of native and carboxylated agarose gels.<sup>75</sup> Recently, ROA has been applied to dimannosides with different glycosidic linkages.<sup>76</sup>

Circular dichroism (CD) is a well-established technique in peptide science that provides a characteristic fingerprint for each secondary structure. In polysaccharides, the absence of chromophores limits the use of this technique. Even in the carboxylate containing xanthan, CD spectroscopy lacks sensitivity to detect differences in the local conformation. Furthermore, the carboxylic chromophore, located in the sidechain, might not be informative of the backbone conformation.<sup>77</sup> In contrast, CD analysis proved useful to monitor the conformational transition mediated by  $\text{Ca}^{2+}$  ions in oligo and polysialic acid chains.<sup>78</sup> To overcome the lack of a

chromophore, Induced Circular Dichroism (ICD) has been applied. ICD occurs when a chromophore, such as Congo Red, binds to a polysaccharide arranged in a particular ordered structure, inducing CD signals at higher wavelengths. The appearance of CD bands is related to the ordered arrangement of the bound chromophore. Additionally, staining with Congo Red reveals the presence of an ordered secondary structure, resulting in a redshift of the absorption maximum ( $\lambda_{\text{max}}$ ) in the UV-Vis spectrum of Congo Red.<sup>79</sup> An alternative for unsubstituted polysaccharides (e.g. amylose), in which no electronic transition above 190 nm is present, is Vacuum Ultraviolet Circular Dichroism (VUCD). VUCD enable conformational studies, exploiting higher energy electronic transitions, typical of the ether chromophore. Nevertheless, the need for intense vacuum UV sources (i.e. synchrotron radiation) and the rather challenging results interpretation limited the use of this technique.

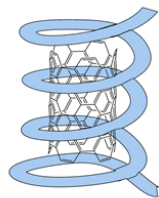
Other techniques such as size exclusion chromatography (SEC), calorimetry, viscosity or viscoelastic measurements, and electric birefringence have been employed to gain insight into macromolecular conformations. Nevertheless, interpreting the results is difficult and usually debatable, as is the case for xanthan secondary structure.<sup>38,50</sup>

#### 4 HELICAL STABILIZATION

The intrinsic flexibility of polysaccharides was often associated with a lack of a stable secondary structure.<sup>70</sup> Despite the flexibility, polysaccharides' helical character is deeply involved in the interaction with themselves or other substances, affecting their overall macroscopic properties. The ability to control the conformation of these molecules is therefore desirable to achieve control over their function. Several ways to stabilize the helical secondary structure have been proposed, based on intra- or intermolecular strategies (Figure 5). Supramolecular complexation of hydrophobic guests stabilizes the central cavity of helical structures. Moreover, the helical motif of some polysaccharides triggers the formation of higher hierarchical assemblies, such as gels or defined nanomaterials. Disorder-order transitions can be controlled with external stimuli. In particular, control over the ionic environment (i.e. ion type and concentration) proved to be crucial to control the formation of helical secondary structures, but also higher organization levels, such as tertiary and quaternary structures. Chemical modifications can also stabilize helical conformations, influencing both macroscopic properties and interactions with other molecules. Moreover, double and triple helices can form through intermolecular interactions and represent another approach to stabilize the helical conformation.

#### Section 4.1 Intramolecular stabilization and inclusion complexes

- Guest molecules
- Ionic strength
- Chemical modification



#### Section 4.2 Intermolecular stabilization

- Triple helices
- Chemical modification



#### Section 4.3 Gel formation and aggregation

- Ionic strength
- Supercoiling
- Self-assembly



**Figure 5** Graphic representation of the different approaches to stabilize helical polysaccharides. Adapted from <sup>80</sup> and <sup>6</sup> with permission from the Royal Society of Chemistry.

### 4.1 Intramolecular stabilization and inclusion complexes

#### *Inclusion complexes*

Due to their intrinsic flexibility, several polysaccharides can adapt their helical sizes and wrap around molecular guests. The most established example of intramolecular helical stabilization is represented by the formation of amylose-polyiodide complex. MD simulations show that the single helix of V-amylose is not stable in water, nor in DMSO, since hydrogen bonds are not strong enough to maintain the single helix shape.<sup>17</sup> However, when a single polyiodide chain is located in the hydrophobic cavity of V-amylose, extra stabilization can be gained from hydrophobic interactions, which stabilize the cavity of the hollow helix.<sup>81</sup> This inclusion complex is commonly exploited for the colorimetric detection of starch (iodine test) or for iodometric titrations. Following this approach, many stable supramolecular inclusion complexes have been reported.

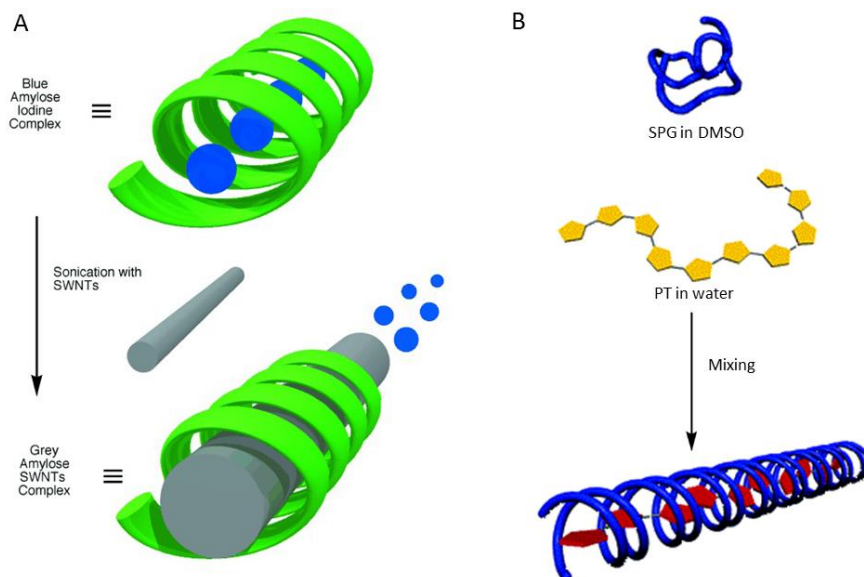


**Figure 6** A) Schematic representation of the “pea-shooting” mechanism in which SWNTs replace iodine molecules in the amylose cavity. Reprinted with permission from<sup>8</sup>. B) Schematic illustration of the chiral polythiophene (PT)-schizophyllan (SPG) inclusion complex. Adapted with permission from<sup>82</sup>. Copyright 2005 American Chemical Society.

Cyclic oligosaccharides such as cyclodextrins (CDs) have a torus-like shape with a hydrophilic exterior and an hydrophobic central cavity, prone to include guest molecules (e.g. fullerene/ $\beta$ -CD complex).<sup>83–86</sup> Following the same idea, single walled nanotubes (SWNTs) have been wrapped with amylose, the macromolecular linear analogue of CDs. Upon wrapping, the poorly soluble SWNTs become water soluble and more biocompatible, expanding their potential to biological applications. The formation of the SWNTs-amylose complex proceeds through a “pea-shooting” or insertion mechanism, in which the SWNT replaces the guest in a prearranged iodine-amylose complex (Figure 6A). Eventually, the SWNTs can be released following enzymatic hydrolysis of the polysaccharide, which allows for this process to be used as a purification protocol for SWNTs.<sup>8</sup> An alternative complexation mechanism follows a cooperative binding of SWNTs to amylose, in a loosely elongated helical state. In this wrapping mechanism, no prearranged helical amylose is needed. Suitable solvent mixtures (i.e. DMSO/water) and powerful sonication are key factors for the formation of inclusion complexes. The glycosidic linkage plays an important role, since pullulan, which has an  $\alpha$ -1,6 linkage every second  $\alpha$ -1,4 glucose unit, showed lower encapsulating abilities. This observation was ascribed to the  $\alpha$ -1,6 glycosidic bond that induces a partial kink, hindering the formation of long helical regions.<sup>87</sup>

$\beta$ -1,3 Glucans, such as schizophyllan and curdlan, have a strong tendency to form helices, wrapping linear guest molecules, such as carbon nanotubes. These polysaccharides are denatured in DMSO, while they tend to fold into triple helices in water. By mixing an aqueous suspension of SWNTs with a DMSO solution of curdlan or schizophyllan, it is possible to generate inclusion complexes, which stabilize well-dispersed fibrils of SWNTs preventing their aggregation. NIR-Vis and Raman spectroscopy confirmed the formation of the inclusion complex and the periodical helical superstructure was observed with TEM and AFM imaging. Among all polyglucosides, schizophyllan showed the best results for the formation of a stable complex with as-grown SWNTs. In this system, two schizophyllan chains are wrapped around a single piece of as-grown SWNT.<sup>23</sup> Even the mostly linear cellulose has been reported to wrap SWNTs upon sonication or using an ionic liquid-assisted preparation.<sup>88,89</sup> MD simulations showed that the ability to form intramolecular hydrogen bonds, as well as to orient the pyranose rings parallel to the surface of the SWNT, are key factors that regulate the interaction with the hydrophobic guest.<sup>90</sup> However, further improvement of theoretical models is needed to correlate the results of MD simulations to experimental data. Other SWNTs-polysaccharide inclusion complexes have been reported, based on chitosan and alginate, respectively positively and negatively charged. The different ratio of the charged polysaccharides tunes the  $\zeta$  potential of the SWCNTs.<sup>91</sup>

The hydrophobic cavity of schizophyllan is accessible only after denaturation, allowing either for the formation of inclusion complexes or co-helices. Various polymeric guests have been mixed with schizophyllan, giving rise to different supramolecular architectures. These include conjugated polymers, such as polyaniline (PANI)<sup>92</sup>, permethyldecasilane (PMDS)<sup>93</sup>, and polythiophene (PT)<sup>82</sup>. PT resulted in a co-helix assembly, while inclusion complexes were formed with the other guests. In this kind of “molecular wires” the entrapped polymers show chiral twisting, reflecting the host’s chirality (Figure 6B). Carboxymethylated amylose (left-handed helix) and schizophyllan (right-handed helix) form inclusion complexes with oligosilanes,

inducing left- or right-handed twisting respectively.<sup>94</sup> Structural changes of the guest occurring inside the cavity can also be induced by external stimuli. Interestingly, an inclusion complex of modified curdlan with PT showed thermo and solvent responsive behavior, due to the helical rearrangement of the guest entrapped in the cavity.<sup>95</sup>

Inclusion complexes could be also obtained upon synthesis of the guest molecule inside the cavity of the helical polysaccharide, as shown for the amylose-polystyrene (PS) complex. The styrene monomer is placed inside the amylose cavity before free radical polymerization takes place.<sup>96</sup> As an alternative to obtain the corresponding inclusion complex, the inverse approach, called “vine-twining polymerization”, features the enzymatic synthesis of amylose in the presence of polytetrahydrofuran (polyTHF).<sup>97</sup>

The wrapping tendency of polysaccharides was exploited for the generation of SWNTs-Au hybrid nanomaterials. A bilayer of alginate and chitosan wrapped around SWNTs allowed for the amino and carboxylic acid moieties to function as active metal-binding groups around the SWNTs. Subsequent *in situ* reduction of HAuCl<sub>4</sub> resulted in gold nanoparticle coated SWNTs, with potential application for photothermal therapy.<sup>98</sup> Linear clusters were also obtained aligning in a monodimensional arrangement of gold nanoparticles in the hollow helix of schizophyllan.<sup>99</sup>

#### *Chemical modification*

Chemical modification proved to be a valuable approach to improve helical stability. Both the backbone and side chains can be modified with many strategies for regioselective functionalization.<sup>100–102</sup> Introduction of charged groups, recognition appendages or aromatic moieties, are key tools to favor the formation of helical domains, affecting the interaction with other entities (*i.e.* SWNTs, lectins). The stabilization obtained through chemical modification can rigidify the single helical structure, preventing the formation of intermolecular assemblies, as in the case of a branched  $\beta$ -1,3 glucan extracted from baker's yeast. Formylation was used to destabilize the native triple helix and convert it to a single stranded helix.<sup>79</sup>

The selective introduction of a positively charged sidechain at the C-6 position of curdlan, originally designed to overcome water insolubility, strongly influences curdlan native conformation. The standard curdlan triple helix is converted into a single stranded helix that maintains the hydrophobic cavity and is able to complex guest molecules (*i.e.* SWNTs, PMDS), via an induced-fit mechanism. The cationic appendages provide attractive electrostatic interactions, which stabilize complexation of cationic curdlan with poly(C).<sup>103</sup> Functionalization of polysaccharide inclusion complexes was also exploited for recognition. Lactoside appended schizophyllan permitted to wrap SWNTs to gain water solubility as well as selective lectin binding.<sup>104</sup> The chemical introduction of aromatic moieties on dextran, an  $\alpha$ -1,6 glucan, enhances the interaction with SWNTs, due to  $\pi$ - $\pi$  stacking. Precise control over the number of aromatic substituents (*i.e.* 13.6 %w) is needed to obtain optimal SWNTs dispersion.<sup>105</sup>

#### *Ion-mediated coil-helix transitions*

The coil-helix transition of biopolymers in solution, common for polypeptides and polynucleotides, is observed also for ionic polysaccharides. Helix formation is usually triggered by temperature lowering, salt addition or solvent exchange. The nature of the residues and the



surrounding ionic environment play an important role in the regulation of the molecular conformation.<sup>106</sup> Moreover, the electrostatic interactions between charges influence folding and aggregation, not only at a single molecule level, but also at higher levels, as demonstrated by the formation of three-dimensional gel networks.

Carrageenans are a class of natural sulfated galactans, extracted from seaweeds that undergo ion-induced helix formation, followed by association of chains into extended networks, responsible for gel formation.<sup>6,33,51,107</sup> The different sulfation patterns of iota- and lambda-carrageenans result in different gelation behavior, upon addition of salt. AFM imaging revealed that, upon addition of NaCl solutions (0 mM to 100 mM), iota-carrageenan undergoes a reversible coil-single helix transition, while lambda-carrageenan maintains the random coil state (Figure 9A and 9B). The increased ionic strength screens the intrachain ionic repulsions of the sulfate groups, resulting in high flexibility of the backbone (lowering the persistence length,  $L_p$ ), which promotes secondary structure formation. New intramolecular hydrogen bonds stabilize the helix.<sup>33</sup> While NaCl and CaCl<sub>2</sub> trigger the formation of single helical secondary structures in iota- and kappa-carrageenans, KCl is able to induce the formation of higher hierarchical assemblies, such as intramolecular supercoiled and intertwined helices (Figure 9C, see section 4.3).<sup>6,107</sup> Magnetic control of macromolecular stiffness and global stretching was achieved following addition of transition metal ions, such as Fe<sup>2+</sup> or Fe<sup>3+</sup>, to iota-carrageenan. The single helix of the Fe<sup>2+</sup>-iota-carrageenan complex showed a 1.5-fold increase in rigidity, upon application of a 1.1 T magnetic field.<sup>108</sup> Tuning the ionic strength of the medium or incorporating magnetic field responsive ions (*i.e.* Fe<sup>2+</sup>) opens up new possibilities to control flexibility, folding, and assembling of carrageenans.

### *Synthesis of tailor-made helical oligosaccharides*

The primary sequence of polypeptides plays a major role in defining the secondary structure. Sequence controlled oligomers (*i.e.* foldamers) can be designed to achieve specific control over the secondary structure. Extremely stable structures resembling natural proteins or with completely new geometries can be obtained, based on relatively short sequences.<sup>109–113</sup> Lack of reliable methods to synthesize well-defined oligo and polysaccharide structures hampered the formation of sugar-based foldamers. Moreover, a detailed structural investigation of such compounds is often missing. Compared to peptide synthesis, the synthesis of oligo- and polysaccharides is more challenging, requiring complex protecting group strategies and precise control over reaction conditions.<sup>114–116</sup> Nevertheless, chemical synthesis remains the only alternative to achieve full control over the oligosaccharide sequence, providing a tool for single-site modifications. *Automated Glycan Assembly (AGA)* allows for the fast assembly of well-defined oligo- and polysaccharide structures (up to a 50-mer<sup>117</sup>), starting from monosaccharide building blocks.<sup>118–121</sup> With this technique, a collection of oligo- and polysaccharides was synthesized and used for structural studies. MD simulations and NMR analysis showed that the different structures adopt different conformations, depending on the glycosidic linkage and the sugar building block. Interestingly, the overall conformation is drastically altered by single-site modification, with great impact on the macroscopic properties of the material (*i.e.* solubility). Surprisingly, even short hexasaccharides adopt a secondary structure that ranges from hollow helix ( $\beta$ -1,6 hexaglycoside), to twisted ribbon (cellulose and chitin hexasaccharides) and random coil ( $\alpha$ -1,6 hexamannoside) (Figure 7).<sup>122</sup>

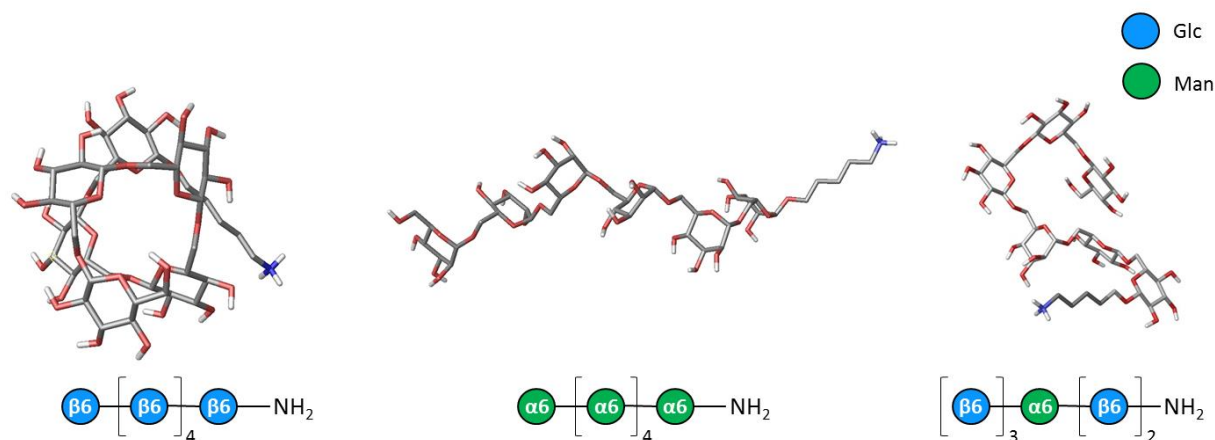


**Figure 7** Global minima conformations obtained from MD simulations for three oligosaccharides. The primary sequence has a marked effect on the conformation and single site substitution completely disrupts the hollow helical conformation of  $\beta$ -1,6 hexagluco-4-amine. Reprinted with permission from<sup>122</sup>. Copyright 2018 American Chemical Society.

In addition to single site substitution, the branching pattern plays an important role in the stabilization of the secondary structure. Recently, a chemoenzymatic approach provided access to tailor-made  $\beta$ -1,4 xylans with defined arabinose branching. It was demonstrated that, while some branching patterns favored crystallinity, others increased cellulose affinity. The latter is the result of the switch between a threefold to a twofold helix arrangement of the arabinoxylan, stabilized by the specific branching pattern.<sup>123,124</sup>

#### 4.2 Intermolecular stabilization

Helical domains of polysaccharides can further associate in a more complex fashion. Triple helices involving distinct polysaccharide molecules result in stable intermolecular complexes.<sup>107</sup> The reversible association permits the formation of hybrid structures able to incorporate polynucleotides for gene delivery applications (Figure 8).

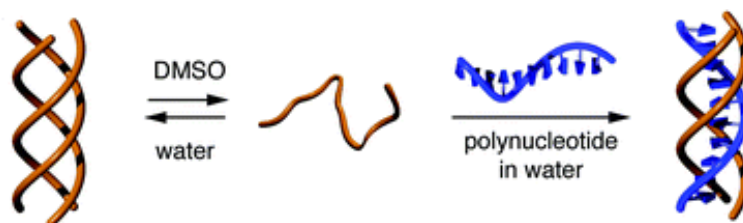


**Figure 8** Solvent-induced conformational transition of curdlan allows for co-helix formation with polynucleotides. Reproduced from<sup>80</sup> with permission from The Royal Society of Chemistry.

The strong tendency of  $\beta$ -1,3 glucans to form triple helices can be exploited to form polysaccharide/polynucleotide complexes. A denaturation process (e.g. exchanging DMSO for water) permits the helix-coil transition of schizophyllan. Single-stranded schizophyllan can be reversibly renatured, by DMSO/water exchange, to recover the native triple helical arrangement. During this renaturing process, molecular guests can be incorporated into the triple co-helix (Figure 8).<sup>92</sup> Incorporation of polynucleotides into hetero-triple helices was reported, with high

selectivity for polynucleotides such as poly(cytidylic acid) and poly(deoxyadenylic acid) (respectively poly(C) and poly(dA)). A well-defined stoichiometric ratio (two polysaccharides per polynucleotide) was obtained.<sup>125–127</sup>

Amphoteric curdlans, bearing both C-6 amino and carboxylic acid moieties generate polypeptide-mimetic with a pH-dependent assembling/disassembling behavior. The triple stranded helix was stable only at pH 2 or 10, while between pH 3 and 9, aggregation followed by precipitation was observed. In contrast, at extremely acidic or basic conditions, the amphoteric curdlan showed single-stranded random coil conformation. The pH responsive conformation switch was applied to capture and release a DNA strand in a controlled manner.<sup>128</sup>

#### 4.3 Polysaccharide-polysaccharide interactions in quaternary structures: gel formation and aggregation

Protein quaternary structure results from non-covalent association of multiple subunits. Large assemblies with structural roles, such as collagen, or smaller self-assembled enzymes demonstrate how quaternary association expands the functions of proteins. Similarly, polysaccharide can self-associate in solution to form gels. The sol-gel transition is a consequence of interchain association, in which specific regions of the polysaccharide backbone associate giving rise to a three dimensional network with viscoelastic behavior (*i.e.* gel). In this process, the helical domains of polysaccharides are often responsible for interchain associations in the junction zones, providing non-covalent crosslinking. Interestingly, the synergistic interactions of different polysaccharide species show a higher quaternary level of association, enhancing the gel properties. Greater gel strength, elasticity and reduced syneresis are observed.<sup>129,130</sup>

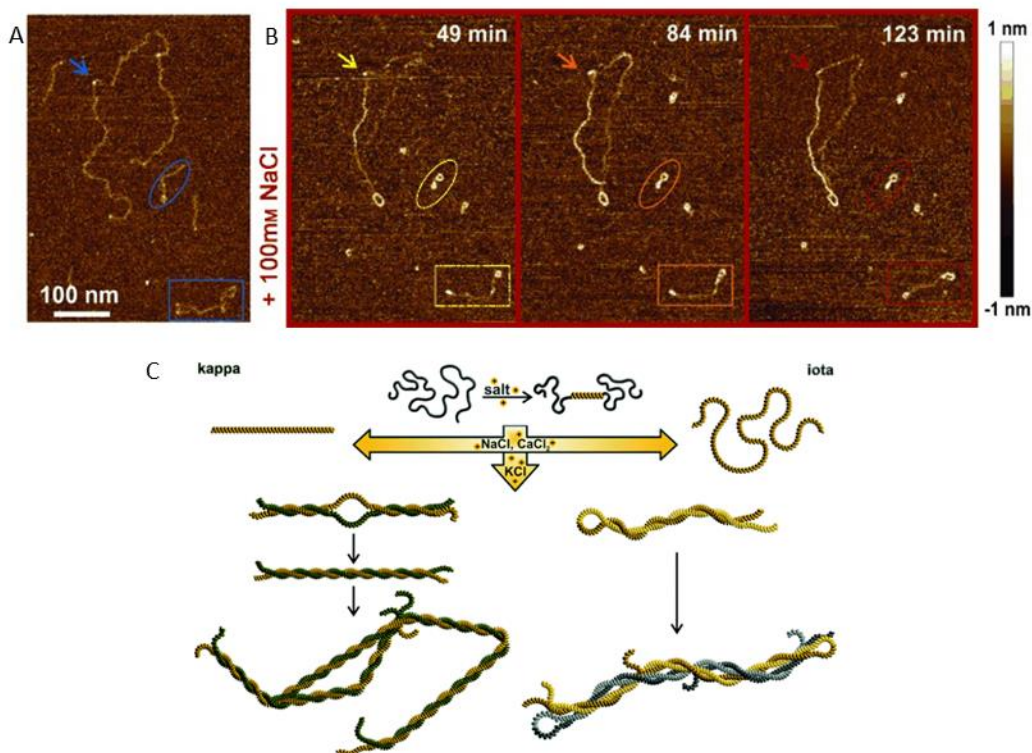


**Figure 9** Ion-mediated coil-helix transition of iota-carrageenan visualized through AFM imaging under liquid conditions A) immersed in MilliQ water and B) after replacement of the liquid environment with 100 mM NaCl solution. The increase in thickness of the single strand with time proves the formation of a single helix. Reprinted with permission from<sup>33</sup>. C) Proposed ion-induced self-assembly mechanism for kappa and iota carrageenans upon addition of NaCl, KCl and CaCl<sub>2</sub>. KCl induces supercoiling and formation of higher hierarchical assemblies. Reproduced from<sup>6</sup> with permission from The Royal Society of Chemistry.

Carrageenans quaternary structures are the results of the intermolecular twisting of secondary structures, which occurs upon addition of salts (*i.e.* ionic strength modulation, Figure 9C). While helical carrageenans such as kappa- and iota- form gels, random coil lambda-carrageenan does not. The unstructured conformation of lambda-carrageenan, resulting from its primary sequence, suppresses helix-helix non-covalent associations.<sup>6,33,107</sup> A similar hierarchical gelation mechanism has been observed also for gellan gum, even though a detailed structural study on other classes of polysaccharides still lacks.

Alginate, an ionic polysaccharide bearing carboxylate groups, undergoes interchain association, upon addition of Ca<sup>2+</sup> ions, giving rise to gel networks. The polyguluronate domains of alginate adopt a buckled-ribbon conformation (*i.e.* 2<sub>1</sub> helix), favoring the interchain association in which divalent cations are complexed by the carboxylate groups.<sup>131</sup>

Polysaccharide-polysaccharide controlled aggregation led to the formation of small objects. The typical triple helical motif of  $\beta$ -1,3 glucans has been exploited as “tiles” to prepare nanostructures with defined shape. Helix-helix interactions were enhanced by acylation (acetylation and formylation) of free hydroxyl groups. These highly rigid triple helical polysaccharides aggregate in solution originating nanosheets. Activation of the “sticky-ends” of these triple helical assemblies provided a way to obtain more complex assemblies, such as nanocapsules.<sup>132</sup>

Chemical modifications can also drive the formation of complex hierarchical assemblies. The formylated branched  $\beta$ -1,3 glucan shows increased stiffness, favoring lateral association leading to formation of rectangular lattices (resembling collagen type I). Multiwalled nanotubes were successfully obtained from self-assembly of lattices and further demonstrate the relevance of interchain interactions.<sup>79</sup> Hierarchical assemblies were also created from the combination of cationic (ammonium) and anionic (sulfate) modified curdlans, wrapped around SWNTs. The two oppositely charged inclusion complexes created a sheet, in which all the building blocks are highly aligned thanks to electrostatic interactions.<sup>133</sup>

## 5 FUTURE PROSPECTS AND CONCLUSIONS

Similarly to polypeptides and polynucleotides, the helical shape is a highly recurrent secondary structure in polysaccharides, strongly affecting their function. Single, double and triple helices with diverse geometrical properties were reported. Many internal factors such as the type of monosaccharide, the glycosidic linkage, the presence of ionic moieties or sidechains, and the branching pattern influence the conformation. In addition, external factors such as ionic environment, pH, and temperature greatly affect the polysaccharide conformation. The intrinsic flexibility of polysaccharides gives rise to high structural variability and, as a consequence, complicates structural studies in solution. Much effort has been dedicated to define the conformation in solution, however, to date, it remains in many cases elusive, hampering the

structure-function correlation. Many analytical techniques, routinely used for protein structural studies, were adapted to polysaccharides, even though often with unsatisfactory results. In most cases, only the solid phase conformation is accessible. Analytical techniques, such as AFM imaging, SMFS, SAXS, and NMR are evolving, with the aim to probe the polysaccharides conformation in solution. The combination of different techniques proved to be highly beneficial, especially when theoretical models (*i.e.* MD simulations) are combined with experimental data. Nevertheless, new analytical techniques are fundamental to get insights into the three-dimensional structure of polysaccharides in solution, key to a better understanding of structure-function relationship. Limited access to pure samples, due to challenging chemical synthesis, has also hampered the development of polysaccharide science. With the development of new synthetic techniques, well-defined sequences became accessible as probes for structure elucidation. Such well-defined structures will fuel the study of the interactions of polysaccharides with themselves as well as with other materials. New insights into aggregation behavior and supramolecular assembly are expected.

The tendency of polysaccharide to form helices and to wrap around guests opened the way to new supramolecular inclusion complexes. This behavior, common for peptide-based foldamers, can be exploited for molecular recognition.<sup>134</sup> Moreover, in analogy to synthetic foldamers,<sup>109–113</sup> chemical modifications permit to greatly influence the conformational behavior to create shape-persistent complex polysaccharides, able to self-assemble into tailor-made nanomaterials. Due to their high biocompatibility and natural abundance, carbohydrate based nanomaterials have great potential for nanotechnology applications. Molecular recognition and catalysis are two of the main fields that could benefit from these new materials. One step in this direction has recently been made; helical polysaccharides were recently applied for molecular recognition of drugs in aqueous solution.<sup>135</sup> In addition, the application of polysaccharides in photochirogenesis has been reported, in which the polysaccharide helical structure, intrinsically chiral, is exploited to achieve stereocontrol.<sup>136</sup> Following this pioneering work, new functional carbohydrate based materials are envisioned.

## ACKNOWLEDGEMENTS

We thank the Max-Planck Society, the Minerva-Fast-Track Program (M.D.), and the MPG-FhG Cooperation Project Glyco3Display (M.D. and G.F.) for generous financial support. We thank Theodore Tyrikos-Ergas, Ankush Singhal and Francesca Fittolani for the help with graphics and images.

## CONFLICT OF INTERESTS

The authors declare no competing financial interests.

## REFERENCES

- (1) Varki A, Cummings RD, Esko JD, et al., E. *Essentials of Glycobiology*, 3rd ed.; Cold



Spring Harbor Laboratory Press: Cold Spring Harbor (NY), 2017.

- (2) Bonduelle, C. Secondary Structures of Synthetic Polypeptide Polymers. *Polym. Chem.* **2018**, 9 (13), 1517–1529. <https://doi.org/10.1039/C7PY01725A>.
- (3) Rees, D. A. *Polysaccharide Shapes*; Springer Netherlands: Dordrecht, 1977. <https://doi.org/10.1007/978-94-011-6906-6>.
- (4) Baek, J. Y.; Geissner, A.; Rathwell, D. C. K.; Meierhofer, D.; Pereira, C. L.; Seeberger, P. H. A Modular Synthetic Route to Size-Defined Immunogenic Haemophilus Influenzae b Antigens Is Key to the Identification of an Octasaccharide Lead Vaccine Candidate. *Chem. Sci.* **2018**, 9 (5), 1279–1288. <https://doi.org/10.1039/C7SC04521B>.
- (5) Rao, V. S. Raghavendra Balaji, Petety V. Chandrasekaran, R. *Conformation of Carbohydrates*; Harwood: Amsterdam, 1998.
- (6) Schefer, L.; Adamcik, J.; Diener, M.; Mezzenga, R. Supramolecular Chiral Self-Assembly and Supercoiling Behavior of Carrageenans at Varying Salt Conditions. *Nanoscale* **2015**, 7 (39), 16182–16188. <https://doi.org/10.1039/c5nr04525h>.
- (7) Rees, D. A.; Welsh, E. J. Secondary and Tertiary Structure of Polysaccharides in Solutions and Gels. *Angew. Chem. Int. Ed.* **1977**, 16 (4), 214–224. <https://doi.org/10.1002/anie.197702141>.
- (8) Alexander, S.; W., S. D.; R., H. J.; Fraser, S. J. Starched Carbon Nanotubes. *Angew. Chem. Int. Ed.* **2002**, 41 (14), 2508–2512. [https://doi.org/10.1002/1521-3773\(20020715\)41:14<2508::AID-ANIE2508>3.0.CO;2-A](https://doi.org/10.1002/1521-3773(20020715)41:14<2508::AID-ANIE2508>3.0.CO;2-A).
- (9) Varki, A.; Cummings, R. D.; Aebi, M.; Packer, N. H.; Seeberger, P. H.; Esko, J. D.; Stanley, P.; Hart, G.; Darvill, A.; Kinoshita, T.; et al. Symbol Nomenclature for Graphical Representations of Glycans. *Glycobiology* **2015**, 25 (12), 1323–1324. <https://doi.org/10.1093/glycob/cwv091>.
- (10) Imberty, A.; Chanzy, H.; Pérez, S.; Buléon, A.; Tran, V. New Three-Dimensional Structure for A-Type Starch. *Macromolecules* **1987**, 20 (10), 2634–2636. <https://doi.org/10.1021/ma00176a054>.
- (11) Imberty, A.; Chanzy, H.; Pérez, S.; Buléon, A.; Tran, V. The Double-Helical Nature of the Crystalline Part of A-Starch. *J. Mol. Biol.* **1988**, 201 (2), 365–378. [https://doi.org/10.1016/0022-2836\(88\)90144-1](https://doi.org/10.1016/0022-2836(88)90144-1).
- (12) Imberty, A.; Perez, S. A Revisit to the Three-Dimensional Structure of B-Type Starch. *Biopolymers* **1988**, 27 (8), 1205–1221. <https://doi.org/10.1002/bip.360270803>.
- (13) Hinrics, W.; Buettner, G.; Steifa, M.; Betzel, C.; Zabel, V.; Pfannemueller, B.; Saenger, W. An Amylose Antiparallel Double Helix at Atomic Resolution. *Science* **1987**, 238 (4824), 205–208. <https://doi.org/10.1126/SCIENCE.238.4824.205>.
- (14) Yamashita, Y.; Hirai, N. Single Crystals of Amylose V Complexes. II. Crystals with 71 Helical Configuration. *J. Polym. Sci. Part A-2 Polym. Phys.* **1966**, 4 (2), 161–171. <https://doi.org/10.1002/pol.1966.160040201>.
- (15) Yamashita, Y.; Monobe, K. Single Crystals of Amylose V Complexes. III. Crystals with 81 Helical Configuration. *J. Polym. Sci. Part A-2 Polym. Phys.* **1971**, 9 (8), 1471–1481. <https://doi.org/10.1002/pol.1971.160090807>.



- (16) Hirai, T.; Hirai, M.; Hayashi, S.; Ueki, T. Study of the Conformational Change of Amylose Induced by Complexation with Iodine Using Synchrotron X-Ray Small-Angle Scattering. *Macromolecules* **1992**, *25* (24), 6699–6702. <https://doi.org/10.1021/ma00050a047>.
- (17) Tusch, M.; Krüger, J.; Fels, G. Structural Stability of V-Amylose Helices in Water-DMSO Mixtures Analyzed by Molecular Dynamics. *J. Chem. Theory Comput.* **2011**, *7* (9), 2919–2928. <https://doi.org/10.1021/ct2005159>.
- (18) Roblin, P.; Potocki-Véronèse, G.; Guieysse, D.; Guerin, F.; Axelos, M.; Perez, J.; Buleon, A. SAXS Conformational Tracking of Amylose Synthesized by Amylosucrases. *Biomacromolecules* **2013**, *14* (1), 232–239. <https://doi.org/10.1021/bm301651y>.
- (19) McIntire, T. M.; Brant, D. A. Observations of the (1→3)- $\beta$ -D-Glucan Linear Triple Helix to Macrocycle Interconversion Using Noncontact Atomic Force Microscopy. *J. Am. Chem. Soc.* **1998**, *120* (28), 6909–6919. <https://doi.org/10.1021/ja981203e>.
- (20) Chuah, C. T.; Sarko, A.; Deslandes, Y.; Marchessault, R. H. Packing Analysis of Carbohydrates and Polysaccharides. Part 14. Triple-Helical Crystalline Structure of Curdlan and Paramylon Hydrates. *Macromolecules* **1983**, *16* (8), 1375–1382. <https://doi.org/10.1021/ma00242a020>.
- (21) Zhang, L.; Wang, C.; Cui, S.; Wang, Z.; Zhang, X. Single-Molecule Force Spectroscopy on Curdlan: Unwinding Helical Structures and Random Coils. *Nano Lett.* **2003**, *3* (8), 1119–1124. <https://doi.org/10.1021/nl034298d>.
- (22) Bluhm, T. L.; Deslandes, Y.; Marchessault, R. H.; Pérez, S.; Rinaudo, M. Solid-State and Solution Conformation of Scleroglucan. *Carbohydr. Res.* **1982**, *100* (1), 117–130. [https://doi.org/10.1016/S0008-6215\(00\)81030-7](https://doi.org/10.1016/S0008-6215(00)81030-7).
- (23) Numata, M.; Asai, M.; Kaneko, K.; Bae, A. H.; Hasegawa, T.; Sakurai, K.; Shinkai, S. Inclusion of Cut and As-Grown Single-Walled Carbon Nanotubes in the Helical Superstructure of Schizophyllan and Curdlan ( $\beta$ -1,3-Glucans). *J. Am. Chem. Soc.* **2005**, *127* (16), 5875–5884. <https://doi.org/10.1021/ja044168m>.
- (24) Okobira, T.; Miyoshi, K.; Uezu, K.; Sakurai, K.; Shinkai, S. Molecular Dynamics Studies of Side Chain Effect on the  $\beta$ -1,3-D-Glucan Triple Helix in Aqueous Solution. *Biomacromolecules* **2008**, *9* (3), 783–788. <https://doi.org/10.1021/bm700511d>.
- (25) Brauer, D.; Kimmons, T.; Phillips, M. Effects of Management on the Yield and High-Molecular-Weight Polysaccharide Content of Shiitake ( *Lentinula Edodes* ) Mushrooms. *J. Agric. Food Chem.* **2002**, *50* (19), 5333–5337. <https://doi.org/10.1021/jf020080l>.
- (26) Atkins, E. D. T.; Parker, K. D. The Helical Structure of a  $\beta$ -D-1,3-Xylan. *J. Polym. Sci. Part C Polym. Symp.* **1969**, *28* (1), 69–81. <https://doi.org/10.1002/polc.5070280109>.
- (27) Miyoshi, K.; Uezu, K.; Sakurai, K.; Shinkai, S. Inter-Chain and Arrayed Hydrogen Bonds in  $\beta$ -1,3-D-Xylan Triple Helix Predicted by Quantum Mechanics Calculation. *Carbohydr. Polym.* **2006**, *66* (3), 352–356. <https://doi.org/10.1016/j.carbpol.2006.03.026>.
- (28) Lap ík, L.; Lap ík, L.; De Smedt, S.; Demeester, J.; Chabre ek, P. Hyaluronan: Preparation, Structure, Properties, and Applications. *Chem. Rev.* **1998**, *98* (8), 2663–2684. <https://doi.org/10.1021/cr941199z>.
- (29) Atkins, E. D. T.; Sheehan, J. K. Hyaluronates: Relation between Molecular Conformations. *Science* **1973**, *179* (4073), 562–564.

<https://doi.org/10.1126/science.179.4073.562>.

- (30) Winter, W. T.; Arnott, S. Hyaluronic Acid: The Role of Divalent Cations in Conformation and Packing. *J. Mol. Biol.* **1977**, *117* (3), 761–784. [https://doi.org/10.1016/0022-2836\(77\)90068-7](https://doi.org/10.1016/0022-2836(77)90068-7).
- (31) Arnott, S.; Mitra, A. K.; Raghunathan, S. Hyaluronic Acid Double Helix. *J. Mol. Biol.* **1983**, *169* (4), 861–872. [https://doi.org/10.1016/S0022-2836\(83\)80140-5](https://doi.org/10.1016/S0022-2836(83)80140-5).
- (32) Anderson, N. S.; Campbell, J. W.; Harding, M. M.; Rees, D. A.; Samuel, J. W. B. X-Ray Diffraction Studies of Polysaccharide Sulphates: Double Helix Models for  $\kappa$ - and  $\iota$ -Carrageenans. *J. Mol. Biol.* **1969**, *45* (1), 85–97. [https://doi.org/10.1016/0022-2836\(69\)90211-3](https://doi.org/10.1016/0022-2836(69)90211-3).
- (33) Schefer, L.; Adamcik, J.; Mezzenga, R. Unravelling Secondary Structure Changes on Individual Anionic Polysaccharide Chains by Atomic Force Microscopy. *Angew. Chem. Int. Ed.* **2014**, *53* (21), 5376–5379. <https://doi.org/10.1002/anie.201402855>.
- (34) Arnott, S.; Fulmer, A.; Scott, W. E.; Dea, I. C. M.; Moorhouse, R.; Rees, D. A. The Agarose Double Helix and Its Function in Agarose Gel Structure. *J. Mol. Biol.* **1974**, *90* (2), 269–284. [https://doi.org/10.1016/0022-2836\(74\)90372-6](https://doi.org/10.1016/0022-2836(74)90372-6).
- (35) Foord, S. A.; Atkins, E. D. Y. New X-Ray Diffraction Results from Agarose: Extended Single Helix Structures and Implications for Gelation Mechanism. *Biopolymers* **1989**, *28* (8), 1345–1365. <https://doi.org/10.1002/bip.360280802>.
- (36) Medronho, B.; Romano, A.; Miguel, M. G.; Stigsson, L.; Lindman, B. Rationalizing Cellulose (in)Solubility: Reviewing Basic Physicochemical Aspects and Role of Hydrophobic Interactions. *Cellulose* **2012**, *19* (3), 581–587. <https://doi.org/10.1007/s10570-011-9644-6>.
- (37) Sundararajan, P. R.; Rao, V. S. R. Conformational Studies of  $\beta$ -D-1,4'-Xylan. *Biopolymers* **1969**, *8* (3), 305–312. <https://doi.org/10.1002/bip.1969.360080302>.
- (38) Morris, E. R. Ordered Conformation of Xanthan in Solutions and “Weak Gels”: Single Helix, Double Helix – or Both? *Food Hydrocoll.* **2019**, *86*, 18–25. <https://doi.org/10.1016/j.foodhyd.2017.11.036>.
- (39) Sletmoen, M.; Maurstad, G.; Sikorski, P.; Paulsen, B. S.; Stokke, B. T. Characterisation of Bacterial Polysaccharides: Steps towards Single-Molecular Studies. *Carbohydr. Res.* **2003**, *338* (23), 2459–2475. <https://doi.org/10.1016/j.carres.2003.07.007>.
- (40) Brisson, J.; Chanzy, H.; Winter, W. T. The Crystal and Molecular Structure of VHamylose by Electron Diffraction Analysis. *Int. J. Biol. Macromol.* **1991**, *13* (1), 31–39. [https://doi.org/10.1016/0141-8130\(91\)90007-H](https://doi.org/10.1016/0141-8130(91)90007-H).
- (41) <http://polysac3db.cermav.cnrs.fr/>.
- (42) Meisburger, S. P.; Thomas, W. C.; Watkins, M. B.; Ando, N. X-Ray Scattering Studies of Protein Structural Dynamics. *Chem. Rev.* **2017**, *117* (12), 7615–7672. <https://doi.org/10.1021/acs.chemrev.6b00790>.
- (43) Jo, S.; Myatt, D.; Qi, Y.; Douth, J.; Clifton, L. A.; Im, W.; Widmalm, G. Multiple Conformational States Contribute to the 3D Structure of a Glucan Decasaccharide: A Combined SAXS and MD Simulation Study. *J. Phys. Chem. B* **2018**, *122* (3), 1169–1175.

<https://doi.org/10.1021/acs.jpcc.7b11085>.

- (44) Gamini, A.; Mandel, M. Physicochemical Properties of Aqueous Xanthan Solutions: Static Light Scattering. *Biopolymers* **1994**, *34* (6), 783–797. <https://doi.org/10.1002/bip.360340610>.
- (45) Wang, J.; Nie, S. Application of Atomic Force Microscopy in Microscopic Analysis of Polysaccharide. *Trends Food Sci. Technol.* **2018**, No. August 2017, 0–1. <https://doi.org/10.1016/j.tifs.2018.02.005>.
- (46) Rajendran, A.; Endo, M.; Sugiyama, H. State-of-the-Art High-Speed Atomic Force Microscopy for Investigation of Single-Molecular Dynamics of Proteins. *Chem. Rev.* **2014**, *114* (2), 1493–1520. <https://doi.org/10.1021/cr300253x>.
- (47) Iwata, K.; Yamazaki, S.; Mutombo, P.; Hapala, P.; Ondřík, M.; Jelínek, P.; Sugimoto, Y. Chemical Structure Imaging of a Single Molecule by Atomic Force Microscopy at Room Temperature. *Nat. Commun.* **2015**, *6* (1), 7766. <https://doi.org/10.1038/ncomms8766>.
- (48) Ando, T. High-Speed Atomic Force Microscopy and Its Future Prospects. *Biophys. Rev.* **2018**, *10* (2), 285–292. <https://doi.org/10.1007/s12551-017-0356-5>.
- (49) Usov, I.; Mezzenga, R. FiberApp: An Open-Source Software for Tracking and Analyzing Polymers, Filaments, Biomacromolecules, and Fibrous Objects. *Macromolecules* **2015**, *48* (5), 1269–1280. <https://doi.org/10.1021/ma502264c>.
- (50) Camesano, T. A.; Wilkinson, K. J. Single Molecule Study of Xanthan Conformation Using Atomic Force Microscopy. *Biomacromolecules* **2001**, *2* (4), 1184–1191. <https://doi.org/10.1021/bm015555g>.
- (51) Schefer, L.; Usov, I.; Mezzenga, R. Anomalous Stiffening and Ion-Induced Coil-Helix Transition of Carrageenans under Monovalent Salt Conditions. *Biomacromolecules* **2015**, *16* (3), 985–991. <https://doi.org/10.1021/bm501874k>.
- (52) Rief, M.; Oesterhelt, F.; Heymann, B.; Gaub, H. E. Single Molecule Force Spectroscopy on Polysaccharides by Atomic Force Microscopy. *Science* **1997**, *275* (5304), 1295–1297. <https://doi.org/10.1126/science.275.5304.1295>.
- (53) Li, H.; Rief, M.; Oesterhelt, F.; Gaub, H. E. Single-Molecule Force Spectroscopy on Xanthan by AFM. *Adv. Mater.* **1998**, *10* (4), 316–319. [https://doi.org/10.1002/\(SICI\)1521-4095\(199803\)10:4<316::AID-ADMA316>3.0.CO;2-A](https://doi.org/10.1002/(SICI)1521-4095(199803)10:4<316::AID-ADMA316>3.0.CO;2-A).
- (54) Jacobs, M. J.; Blank, K. Joining Forces: Integrating the Mechanical and Optical Single Molecule Toolkits. *Chem. Sci.* **2014**, *5* (5), 1680–1697. <https://doi.org/10.1039/C3SC52502C>.
- (55) Bull, M. S.; Sullan, R. M. A.; Li, H.; Perkins, T. T. Improved Single Molecule Force Spectroscopy Using Micromachined Cantilevers. *ACS Nano* **2014**, *8* (5), 4984–4995. <https://doi.org/10.1021/nn5010588>.
- (56) Zhang, Q.; Lu, Z.; Hu, H.; Yang, W.; Marszalek, P. E. Direct Detection of the Formation of V-Amylose Helix by Single Molecule Force Spectroscopy. *J. Am. Chem. Soc.* **2006**, *128* (29), 9387–9393. <https://doi.org/10.1021/ja057693+>.
- (57) Zhang, Q.; Jaroniec, J.; Lee, G.; Marszalek, P. E. Direct Detection of Inter-Residue Hydrogen Bonds in Polysaccharides by Single-Molecule Force Spectroscopy. *Angew.*

- Chem. Int. Ed.* **2005**, *44* (18), 2723–2727. <https://doi.org/10.1002/anie.200462067>.
- (58) Wormald, M. R.; Petrescu, A. J.; Pao, Y.-L.; Glithero, A.; Elliott, T.; Dwek, R. A. Conformational Studies of Oligosaccharides and Glycopeptides: Complementarity of NMR, X-Ray Crystallography, and Molecular Modelling. *Chem. Rev.* **2002**, *102* (2), 371–386. <https://doi.org/10.1021/cr990368i>.
- (59) Patel, D. S.; Pendrill, R.; Mallajosyula, S. S.; Widmalm, G.; MacKerell, A. D. Conformational Properties of  $\alpha$ - or  $\beta$ -(1→6)-Linked Oligosaccharides: Hamiltonian Replica Exchange MD Simulations and NMR Experiments. *J. Phys. Chem. B* **2014**, *118* (11), 2851–2871. <https://doi.org/10.1021/jp412051v>.
- (60) Prestegard, J. H.; Bougault, C. M.; Kishore, A. I. Residual Dipolar Couplings in Structure Determination of Biomolecules. *Chem. Rev.* **2004**, *104* (8), 3519–3540. <https://doi.org/10.1021/cr030419i>.
- (61) Battistel, M. D.; Pendrill, R.; Widmalm, G.; Freedberg, D. I. Direct Evidence for Hydrogen Bonding in Glycans: A Combined NMR and Molecular Dynamics Study. *J. Phys. Chem. B* **2013**, *117* (17), 4860–4869. <https://doi.org/10.1021/jp400402b>.
- (62) Battistel, M. D.; Shangold, M.; Trinh, L.; Shiloach, J.; Freedberg, D. I. Evidence for Helical Structure in a Tetramer of A2-8 Sialic Acid: Unveiling a Structural Antigen. *J. Am. Chem. Soc.* **2012**, *134* (26), 10717–10720. <https://doi.org/10.1021/ja300624j>.
- (63) Almond, A.; Bunkenborg, J.; Franch, T.; Gottfredsen, C. H.; Duus, J. Ø. Comparison of Aqueous Molecular Dynamics with NMR Relaxation and Residual Dipolar Couplings Favors Internal Motion in a Mannose Oligosaccharide. *J. Am. Chem. Soc.* **2001**, *123* (20), 4792–4802. <https://doi.org/10.1021/ja0025696>.
- (64) Rönnols, J.; Engström, O.; Schnupf, U.; Säwén, E.; Brady, J. W.; Widmalm, G. Interresidual Hydrogen Bonding in Carbohydrates Unraveled by NMR Spectroscopy and Molecular Dynamics Simulations. *ChemBioChem* **2019**, cbic.201900301. <https://doi.org/10.1002/cbic.201900301>.
- (65) Dupree, R.; Simmons, T. J.; Mortimer, J. C.; Patel, D.; Iuga, D.; Brown, S. P.; Dupree, P. Probing the Molecular Architecture of *Arabidopsis Thaliana* Secondary Cell Walls Using Two- and Three-Dimensional  $^{13}\text{C}$  Solid State Nuclear Magnetic Resonance Spectroscopy. *Biochemistry* **2015**, *54* (14), 2335–2345. <https://doi.org/10.1021/bi501552k>.
- (66) Canales, Á.; Mallagaray, Á.; Berbís, M. Á.; Navarro-Vázquez, A.; Domínguez, G.; Cañada, F. J.; André, S.; Gabius, H.-J.; Pérez-Castells, J.; Jiménez-Barbero, J. Lanthanide-Chelating Carbohydrate Conjugates Are Useful Tools To Characterize Carbohydrate Conformation in Solution and Sensitive Sensors to Detect Carbohydrate–Protein Interactions. *J. Am. Chem. Soc.* **2014**, *136* (22), 8011–8017. <https://doi.org/10.1021/ja502406x>.
- (67) Canales, A.; Mallagaray, A.; Pérez-Castells, J.; Boos, I.; Unverzagt, C.; André, S.; Gabius, H.-J.; Cañada, F. J.; Jiménez-Barbero, J. Breaking Pseudo-Symmetry in Multiantennary Complex N-Glycans Using Lanthanide-Binding Tags and NMR Pseudo-Contact Shifts. *Angew. Chem. Int. Ed.* **2013**, *52* (51), 13789–13793. <https://doi.org/10.1002/anie.201307845>.
- (68) Martín-Pastor, M.; Canales, A.; Corzana, F.; Asensio, J. L.; Jiménez-Barbero, J. Limited Flexibility of Lactose Detected from Residual Dipolar Couplings Using Molecular



- Dynamics Simulations and Steric Alignment Methods. *J. Am. Chem. Soc.* **2005**, *127* (10), 3589–3595. <https://doi.org/10.1021/ja043445m>.
- (69) Zhang, W.; Meredith, R.; Yoon, M.-K.; Wang, X.; Woods, R. J.; Carmichael, I.; Serianni, A. S. Synthesis and O -Glycosidic Linkage Conformational Analysis of 13 C-Labeled Oligosaccharide Fragments of an Antifreeze Glycolipid. *J. Org. Chem.* **2019**, *acs.joc.8b01411*. <https://doi.org/10.1021/acs.joc.8b01411>.
- (70) Woods, R. J. Predicting the Structures of Glycans, Glycoproteins, and Their Complexes. *Chem. Rev.* **2018**, *118* (17), 8005–8024. <https://doi.org/10.1021/acs.chemrev.8b00032>.
- (71) Berglund, J.; Angles d'Ortoli, T.; Vilaplana, F.; Widmalm, G.; Bergensträhle-Wohlert, M.; Lawoko, M.; Henriksson, G.; Lindström, M.; Wohlert, J. A Molecular Dynamics Study of the Effect of Glycosidic Linkage Type in the Hemicellulose Backbone on the Molecular Chain Flexibility. *Plant J.* **2016**, *88* (1), 56–70. <https://doi.org/10.1111/tpj.13259>.
- (72) Sarkar, A.; Fontana, C.; Imberty, A.; Pérez, S.; Widmalm, G. Conformational Preferences of the O-Antigen Polysaccharides of Escherichia Coli O5ac and O5ab Using NMR Spectroscopy and Molecular Modeling. *Biomacromolecules* **2013**, *14* (7), 2215–2224. <https://doi.org/10.1021/bm400354y>.
- (73) Wu, E. L.; Engström, O.; Jo, S.; Stuhlsatz, D.; Yeom, M. S.; Klauda, J. B.; Widmalm, G.; Im, W. Molecular Dynamics and NMR Spectroscopy Studies of E. Coli Lipopolysaccharide Structure and Dynamics. *Biophys. J.* **2013**, *105* (6), 1444–1455. <https://doi.org/10.1016/j.bpj.2013.08.002>.
- (74) Toukach, F. V.; Ananikov, V. P. Recent Advances in Computational Predictions of NMR Parameters for the Structure Elucidation of Carbohydrates: Methods and Limitations. *Chem. Soc. Rev.* **2013**, *42* (21), 8376. <https://doi.org/10.1039/c3cs60073d>.
- (75) Rütther, A.; Forget, A.; Roy, A.; Carballo, C.; Mießmer, F.; Dukor, R. K.; Nafie, L. A.; Johannessen, C.; Shastri, V. P.; Lüdeke, S. Unravelling a Direct Role for Polysaccharide  $\beta$ -Strands in the Higher Order Structure of Physical Hydrogels. *Angew. Chem.* **2017**, *129* (16), 4674–4678. <https://doi.org/10.1002/ange.201701019>.
- (76) Pendrill, R.; Mutter, S. T.; Mensch, C.; Barron, L. D.; Blanch, E. W.; Popelier, P. L. A.; Widmalm, G.; Johannessen, C. Solution Structure of Mannobioses Unravelling by Means of Raman Optical Activity. *ChemPhysChem* **2019**, *20* (5), 695–705. <https://doi.org/10.1002/cphc.201801172>.
- (77) Capron, I.; Brigand, G.; Muller, G. About the Native and Renatured Conformation of Xanthan Exopolysaccharide. *Polymer* **1997**, *38* (21), 5289–5295. [https://doi.org/10.1016/S0032-3861\(97\)00079-7](https://doi.org/10.1016/S0032-3861(97)00079-7).
- (78) Shimoda, Y.; Kitajima, K.; Inoue, S.; Inoue, Y. Calcium Ion Binding of Three Different Types of Oligo/Polysialic Acids As Studied by Equilibrium Dialysis and Circular Dichroic Methods. *Biochemistry* **1994**, *33* (5), 1202–1208. <https://doi.org/10.1021/bi00171a020>.
- (79) Wu, C.; Wang, X.; Chu, B.; Tang, S.; Wang, Y. Self-Assembly of Core-Corona  $\beta$ -Glucan into Stiff and Metalizable Nanostructures from 1D to 3D. *ACS Nano* **2018**, *12* (10), 10545–10553. <https://doi.org/10.1021/acsnano.8b06560>.
- (80) Hasegawa, T.; Numata, M.; Okumura, S.; Kimura, T.; Sakurai, K.; Shinkai, S. Carbohydrate-Appended Curdlans as a New Family of Glycoclusters with Binding Properties Both for a Polynucleotide and Lectins. *Org. Biomol. Chem.* **2007**, *5* (15), 2404–

2412. <https://doi.org/10.1039/b703720a>.

- (81) Rundle, R. E. The Configuration of Starch in the Starch-Iodine Complex. V. Fourier Projections from X-Ray Diagrams 1. *J. Am. Chem. Soc.* **1947**, *69* (7), 1769–1772. <https://doi.org/10.1021/ja01199a054>.
- (82) Li, C.; Numata, M.; Bae, A.-H.; Sakurai, K.; Shinkai, S. Self-Assembly of Supramolecular Chiral Insulated Molecular Wire. *J. Am. Chem. Soc.* **2005**, *127* (13), 4548–4549. <https://doi.org/10.1021/ja050168q>.
- (83) Delbianco, M.; Bharate, P.; Varela-Aramburu, S.; Seeberger, P. H. Carbohydrates in Supramolecular Chemistry. *Chem. Rev.* **2016**, *116* (4), 1693–1752. <https://doi.org/10.1021/acs.chemrev.5b00516>.
- (84) Martínez, Á.; Ortiz Mellet, C.; García Fernández, J. M. Cyclodextrin-Based Multivalent Glycodisplays: Covalent and Supramolecular Conjugates to Assess Carbohydrate–protein Interactions. *Chem. Soc. Rev.* **2013**, *42* (11), 4746. <https://doi.org/10.1039/c2cs35424a>.
- (85) Harada, A.; Takashima, Y.; Nakahata, M. Supramolecular Polymeric Materials via Cyclodextrin–Guest Interactions. *Acc. Chem. Res.* **2014**, *47* (7), 2128–2140. <https://doi.org/10.1021/ar500109h>.
- (86) Crini, G. Review: A History of Cyclodextrins. *Chem. Rev.* **2014**, *114* (21), 10940–10975. <https://doi.org/10.1021/cr500081p>.
- (87) Kim, O. K.; Je, J.; Baldwin, J. W.; Kooi, S.; Pehrsson, P. E.; Buckley, L. J. Solubilization of Single-Wall Carbon Nanotubes by Supramolecular Encapsulation of Helical Amylose. *J. Am. Chem. Soc.* **2003**, *125* (15), 4426–4427. <https://doi.org/10.1021/ja029233b>.
- (88) Li, L.; Meng, L.; Zhang, X.; Fu, C.; Lu, Q. The Ionic Liquid-Associated Synthesis of a Cellulose/SWCNT Complex and Its Remarkable Biocompatibility. *J. Mater. Chem.* **2009**, *19* (22), 3612. <https://doi.org/10.1039/b823322e>.
- (89) Adsul, M. G.; Rey, D. A.; Gokhale, D. V. Combined Strategy for the Dispersion/Dissolution of Single Walled Carbon Nanotubes and Cellulose in Water. *J. Mater. Chem.* **2011**, *21* (7), 2054. <https://doi.org/10.1039/c0jm03186k>.
- (90) Fu, H.; Chipot, C.; Shao, X.; Cai, W. Why Do the Structural Properties of Complexes Formed by Glucans and Carbon Nanotubes Differ so Much? *RSC Adv.* **2015**, *5* (116), 95682–95689. <https://doi.org/10.1039/c5ra17472d>.
- (91) Zhang, X.; Meng, L.; Lu, Q. Cell Behaviors on Polysaccharide-Wrapped Single-Wall Carbon Nanotubes: A Quantitative Study of the Surface Properties of Biomimetic Nanofibrous Scaffolds. *ACS Nano* **2009**, *3* (10), 3200–3206. <https://doi.org/10.1021/nn9006362>.
- (92) Numata, M.; Shinkai, S. “Supramolecular Wrapping Chemistry” by Helix-Forming Polysaccharides: A Powerful Strategy for Generating Diverse Polymeric Nano-Architectures. *Chem. Commun.* **2011**, *47* (7), 1961–1975. <https://doi.org/10.1039/c0cc03133j>.
- (93) Haraguchi, S.; Hasegawa, T.; Numata, M.; Fujiki, M.; Uezu, K.; Sakurai, K.; Shinkai, S. Oligosilane-Nanofibers Can Be Prepared through Fabrication of Permethyldecasilane within a Helical Superstructure of Schizophyllan. *Org. Lett.* **2005**, *7* (25), 5605–5608. <https://doi.org/10.1021/ol052170s>.



- (94) Sanji, T.; Kato, N.; Kato, M.; Tanaka, M. Helical Folding in a Helical Channel: Chiroptical Transcription of Helical Information through Chiral Wrapping. *Angew. Chem. Int. Ed.* **2005**, *44* (44), 7301–7304. <https://doi.org/10.1002/anie.200502073>.
- (95) Shiraki, T.; Dawn, A.; Tsuchiya, Y.; Shinkai, S. Thermo- and Solvent-Responsive Polymer Complex Created from Supramolecular Complexation between a Helix-Forming Polysaccharide and a Cationic Polythiophene. *J. Am. Chem. Soc.* **2010**, *132* (39), 13928–13935. <https://doi.org/10.1021/ja1067349>.
- (96) Kumar, K.; Woortman, A. J. J.; Loos, K. Synthesis of Amylose–Polystyrene Inclusion Complexes by a Facile Preparation Route. *Biomacromolecules* **2013**, *14* (6), 1955–1960. <https://doi.org/10.1021/bm400340k>.
- (97) Kadokawa, J.; Kaneko, Y.; Tagaya, H.; Chiba, K. Synthesis of an Amylose–polymer Inclusion Complex by Enzymatic Polymerization of Glucose 1-Phosphate Catalyzed by Phosphorylase Enzyme in the Presence of PolyTHF: A New Method for Synthesis of Polymer–polymer Inclusion Complexes. *Chem. Commun.* **2001**, *0* (5), 449–450. <https://doi.org/10.1039/b008180i>.
- (98) Meng, L.; Xia, W.; Liu, L.; Niu, L.; Lu, Q. Golden Single-Walled Carbon Nanotubes Prepared Using Double Layer Polysaccharides Bridge for Photothermal Therapy. *ACS Appl. Mater. Interfaces* **2014**, *6* (7), 4989–4996. <https://doi.org/10.1021/am406031n>.
- (99) Bae, A.-H.; Numata, M.; Hasegawa, T.; Li, C.; Kaneko, K.; Sakurai, K.; Shinkai, S. 1D Arrangement of Au Nanoparticles by the Helical Structure of Schizophyllan: A Unique Encounter of a Natural Product with Inorganic Compounds. *Angew. Chem.* **2005**, *117* (13), 2066–2069. <https://doi.org/10.1002/ange.200462810>.
- (100) Fox, S. C.; Li, B.; Xu, D.; Edgar, K. J. Regioselective Esterification and Etherification of Cellulose: A Review. *Biomacromolecules* **2011**, *12* (6), 1956–1972. <https://doi.org/10.1021/bm200260d>.
- (101) Cumpstey, I. Chemical Modification of Polysaccharides. *ISRN Org. Chem.* **2013**, *2013*, 1–27. <https://doi.org/10.1155/2013/417672>.
- (102) Li, S.; Xiong, Q.; Lai, X.; Li, X.; Wan, M.; Zhang, J.; Yan, Y.; Cao, M.; Lu, L.; Guan, J.; et al. Molecular Modification of Polysaccharides and Resulting Bioactivities. *Compr. Rev. Food Sci. Food Saf.* **2016**, *15* (2), 237–250. <https://doi.org/10.1111/1541-4337.12161>.
- (103) Ikeda, M.; Hasegawa, T.; Numata, M.; Sugikawa, K.; Sakurai, K.; Fujiki, M.; Shinkai, S. Instantaneous Inclusion of a Polynucleotide and Hydrophobic Guest Molecules into a Helical Core of Cationic  $\beta$ -1,3-Glucan Polysaccharide. *J. Am. Chem. Soc.* **2007**, *129* (13), 3979–3988. <https://doi.org/10.1021/ja0684343>.
- (104) Hasegawa, T.; Fujisawa, T.; Numata, M.; Umeda, M.; Matsumoto, T.; Kimura, T.; Okumura, S.; Sakurai, K.; Shinkai, S. Single-Walled Carbon Nanotubes Acquire a Specific Lectin-Affinity through Supramolecular Wrapping with Lactose-Appended Schizophyllan. *Chem. Commun.* **2004**, *10* (19), 2150–2151. <https://doi.org/10.1039/b407409b>.
- (105) Kwon, T.; Lee, G.; Choi, H.; Strano, M. S.; Kim, W.-J. Highly Efficient Exfoliation of Individual Single-Walled Carbon Nanotubes by Biocompatible Phenoxylated Dextran. *Nanoscale* **2013**, *5* (15), 6773. <https://doi.org/10.1039/c3nr01352a>.
- (106) van de Velde, F.; Rollema, H. S.; Grinberg, N. V.; Burova, T. V.; Grinberg, V. Y.; Tromp, R. H. Coil-Helix Transition of Iota-Carrageenan as a Function of Chain Regularity.

- Biopolymers* **2002**, *65* (4), 299–312. <https://doi.org/10.1002/bip.10250>.
- (107) Diener, M.; Adamcik, J.; Sánchez-Ferrer, A.; Jaedig, F.; Schefer, L.; Mezzenga, R. Primary, Secondary, Tertiary and Quaternary Structure Levels in Linear Polysaccharides: From Random Coil, to Single Helix to Supramolecular Assembly. *Biomacromolecules* **2019**, *20* (4), 1731–1739. <https://doi.org/10.1021/acs.biomac.9b00087>.
- (108) Schefer, L.; Bulant, A.; Zeder, C.; Saha, A.; Mezzenga, R. Magnetic Control of Macromolecular Conformations in Supramolecular Anionic Polysaccharide-Iron Complexes. *Angew. Chem. Int. Ed.* **2015**, *54* (45), 13289–13292. <https://doi.org/10.1002/anie.201506898>.
- (109) Guichard, G.; Huc, I. Synthetic Foldamers. *Chem. Commun.* **2011**, *47* (21), 5933. <https://doi.org/10.1039/c1cc11137j>.
- (110) Checco, J. W.; Gellman, S. H. Targeting Recognition Surfaces on Natural Proteins with Peptidic Foldamers. *Curr. Opin. Struct. Biol.* **2016**, *39*, 96–105. <https://doi.org/10.1016/j.sbi.2016.06.014>.
- (111) Yoo, S. H.; Lee, H.-S. Foldectures: 3D Molecular Architectures from Self-Assembly of Peptide Foldamers. *Acc. Chem. Res.* **2017**, *50* (4), 832–841. <https://doi.org/10.1021/acs.accounts.6b00545>.
- (112) Kwon, S.; Kim, B. J.; Lim, H.-K.; Kang, K.; Yoo, S. H.; Gong, J.; Yoon, E.; Lee, J.; Choi, I. S.; Kim, H.; et al. Magnetotactic Molecular Architectures from Self-Assembly of  $\beta$ -Peptide Foldamers. *Nat. Commun.* **2015**, *6* (1), 8747. <https://doi.org/10.1038/ncomms9747>.
- (113) Del Borgo, M. P.; Mechler, A. I.; Traore, D.; Forsyth, C.; Wilce, J. A.; Wilce, M. C. J.; Aguilar, M.-I.; Perlmutter, P. Supramolecular Self-Assembly of N -Acetyl-Capped  $\beta$ -Peptides Leads to Nano- to Macroscale Fiber Formation. *Angew. Chem.* **2013**, *125* (32), 8424–8428. <https://doi.org/10.1002/ange.201303175>.
- (114) Mydock, L. K.; Demchenko, A. V. Mechanism of Chemical O-Glycosylation: From Early Studies to Recent Discoveries. *Org. Biomol. Chem.* **2010**, *8* (3), 497–510. <https://doi.org/10.1039/b916088d>.
- (115) Crich, D. Mechanism of a Chemical Glycosylation Reaction. *Acc. Chem. Res.* **2010**, *43* (8), 1144–1153. <https://doi.org/10.1021/ar100035r>.
- (116) Krasnova, L.; Wong, C.-H. Oligosaccharide Synthesis and Translational Innovation. *J. Am. Chem. Soc.* **2019**, *141* (9), 3735–3754. <https://doi.org/10.1021/jacs.8b11005>.
- (117) Naresh, K.; Schumacher, F.; Hahm, H. S.; Seeberger, P. H. Pushing the Limits of Automated Glycan Assembly: Synthesis of a 50mer Polymannoside. *Chem. Commun.* **2017**, *53* (65), 9085–9088. <https://doi.org/10.1039/c7cc04380e>.
- (118) Seeberger, P. H. The Logic of Automated Glycan Assembly. *Acc. Chem. Res.* **2015**, *48* (5), 1450–1463. <https://doi.org/10.1021/ar5004362>.
- (119) Schumann, B.; Hahm, H. S.; Parameswarappa, S. G.; Reppe, K.; Wahlbrink, A.; Govindan, S.; Kaplonek, P.; Pirofski, L.-A.; Witzernath, M.; Anish, C.; et al. A Semisynthetic *Streptococcus Pneumoniae* Serotype 8 Glycoconjugate Vaccine. *Sci. Transl. Med.* **2017**, *9* (380), eaaf5347. <https://doi.org/10.1126/scitranslmed.aaf5347>.
- (120) Pardo-Vargas, A.; Delbianco, M.; Seeberger, P. H. Automated Glycan Assembly as an

- Enabling Technology. *Curr. Opin. Chem. Biol.* **2018**, *46*, 48–55.  
<https://doi.org/10.1016/j.cbpa.2018.04.007>.
- (121) Hahm, H. S.; Broecker, F.; Kawasaki, F.; Mietzsch, M.; Heilbronn, R.; Fukuda, M.; Seeberger, P. H. Automated Glycan Assembly of Oligo-N-Acetyllactosamine and Keratan Sulfate Probes to Study Virus-Glycan Interactions. *Chem* **2017**, *2* (1), 114–124.  
<https://doi.org/10.1016/J.CHEMPR.2016.12.004>.
- (122) Delbianco, M.; Kononov, A.; Poveda, A.; Yu, Y.; Diercks, T.; Jiménez-Barbero, J.; Seeberger, P. H. Well-Defined Oligo- and Polysaccharides as Ideal Probes for Structural Studies. *J. Am. Chem. Soc.* **2018**, *140* (16), 5421–5426.  
<https://doi.org/10.1021/jacs.8b00254>.
- (123) Senf, D.; Ruprecht, C.; Kishani, S.; Matic, A.; Toriz, G.; Gatenholm, P.; Wågberg, L.; Pfrengle, F. Tailormade Polysaccharides with Defined Branching Patterns: Enzymatic Polymerization of Arabinoxylan Oligosaccharides. *Angew. Chem. Int. Ed.* **2018**, *57* (37), 11987–11992. <https://doi.org/10.1002/anie.201806871>.
- (124) Simmons, T. J.; Mortimer, J. C.; Bernardinelli, O. D.; Pöppler, A.-C.; Brown, S. P.; DeAzevedo, E. R.; Dupree, R.; Dupree, P. Folding of Xylan onto Cellulose Fibrils in Plant Cell Walls Revealed by Solid-State NMR. *Nat. Commun.* **2016**, *7* (1), 13902.  
<https://doi.org/10.1038/ncomms13902>.
- (125) Sakurai, K.; Shinkai, S. Molecular Recognition of Adenine, Cytosine, and Uracil in a Single-Stranded RNA by a Natural Polysaccharide: Schizophyllan. *J. Am. Chem. Soc.* **2000**, *122* (18), 4520–4521. <https://doi.org/10.1021/ja0000145>.
- (126) Bae, A. H.; Lee, S. W.; Ikeda, M.; Sano, M.; Shinkai, S.; Sakurai, K. Rod-like Architecture and Helicity of the Poly(C)/Schizophyllan Complex Observed by AFM and SEM. *Carbohydr. Res.* **2004**, *339* (2), 251–258. <https://doi.org/10.1016/j.carres.2003.09.032>.
- (127) Sanada, Y.; Matsuzaki, T.; Mochizuki, S.; Okobira, T.; Uezu, K.; Sakurai, K.  $\beta$ -1,3-D-Glucan Schizophyllan/Poly(DA) Triple-Helical Complex in Dilute Solution. *J. Phys. Chem. B* **2012**, *116* (1), 87–94. <https://doi.org/10.1021/jp209027u>.
- (128) Tamaru, S. I.; Tokunaga, D.; Hori, K.; Matsuda, S.; Shinkai, S. Giant Amino Acids Designed on the Polysaccharide Scaffold and Their Protein-like Structural Interconversion. *Org. Biomol. Chem.* **2014**, *12* (5), 815–822.  
<https://doi.org/10.1039/c3ob41845f>.
- (129) Paradossi, G.; Chiessi, E.; Barbiroli, A.; Fessas, D. Xanthan and Glucomannan Mixtures: Synergistic Interactions and Gelation. *Biomacromolecules* **2002**, *3* (3), 498–504.  
<https://doi.org/10.1021/bm010163v>.
- (130) Abbaszadeh, A.; MacNaughtan, W.; Sworn, G.; Foster, T. J. New Insights into Xanthan Synergistic Interactions with Konjac Glucomannan: A Novel Interaction Mechanism Proposal. *Carbohydr. Polym.* **2016**, *144*, 168–177.  
<https://doi.org/10.1016/j.carbpol.2016.02.026>.
- (131) Braccini, I.; Pérez, S. Molecular Basis of Ca<sup>2+</sup>-Induced Gelation in Alginates and Pectins: The Egg-Box Model Revisited. *Biomacromolecules* **2001**, *2* (4), 1089–1096.  
<https://doi.org/10.1021/bm010008g>.
- (132) Wu, C.; Wang, X.; Wang, J.; Zhang, Z.; Wang, Z.; Wang, Y.; Tang, S. Tile-Based Self-Assembly of a Triple-Helical Polysaccharide into Cell Wall-like Mesoporous

Nanocapsules. *Nanoscale* **2017**, 9 (28), 9938–9945. <https://doi.org/10.1039/c7nr02801f>.

- (133) Numata, M.; Sugikawa, K.; Kaneko, K.; Shinkai, S. Creation of Hierarchical Carbon Nanotube Assemblies through Alternative Packing of Complementary Semi-Artificial  $\beta$ -1,3-Glucan/Carbon Nanotube Composites. *Chem. - A Eur. J.* **2008**, 14 (8), 2398–2404. <https://doi.org/10.1002/chem.200701205>.
- (134) Tanatani, A.; Hughes, T. S.; Moore, J. S. Foldamers as Dynamic Receptors: Probing the Mechanism of Molecular Association between Helical Oligomers and Rodlike Ligands. *Angew. Chem.* **2002**, 114 (2), 335–338. [https://doi.org/10.1002/1521-3757\(20020118\)114:2<335::AID-ANGE335>3.0.CO;2-M](https://doi.org/10.1002/1521-3757(20020118)114:2<335::AID-ANGE335>3.0.CO;2-M).
- (135) Fukuhara, G.; Sasaki, M.; Numata, M.; Mori, T.; Inoue, Y. Oligosaccharide Sensing in Aqueous Media by Porphyrin-Curdlan Conjugates: A Prêt-à-Porter Rather Than Haute-Couture Approach. *Chem. - A Eur. J.* **2017**, 23 (47), 11272–11278. <https://doi.org/10.1002/chem.201701360>.
- (136) Fukuhara, G. Polymer-Based Supramolecular Sensing and Application to Chiral Photochemistry. *Polym. J.* **2015**, 47 (10), 649–655. <https://doi.org/10.1038/pj.2015.52>.

## AUTHOR BIOGRAPHIES

**Giulio Fittolani** obtained his B.Sc. (2016) and M.Sc. (2018) in industrial chemistry from the University of Padua (Italy), with a thesis on fluorinated cellulose analogues. He is currently a Ph.D. candidate at the Max Planck Institute in Potsdam (Germany) in the Carbohydrate Materials group. His current research is centered on the structure of fluorinated oligosaccharides.



**Prof. Peter H. Seeberger** (Ph.D. in biochemistry from U.C. Boulder, U.S.A. and postdoctoral fellow at Sloan-Kettering Cancer Center, U.S.A.) was tenured Associate Professor at MIT (U.S.A.). He then became a Professor at ETH Zurich (Switzerland). He is currently Director at the Max-Planck Institute in Potsdam and Professor at Freie Universität Berlin (Germany). His research covers the glycosciences, from chemistry to immunology.



**Dr Martina Delbianco** obtained her Ph.D. in chemistry at Durham University (U.K.), with a thesis on highly emissive Eu(III) complexes. After two years as a postdoctoral fellow in the group of Prof. Peter H. Seeberger, she became group leader of the Carbohydrate Materials group at the Max-Planck Institute in Potsdam (Germany). Her current research efforts focus on fundamental and applied studies of synthetic oligosaccharide-based materials.

